Long wavelenght inner-resonance cut-off frequencies in elastic composite materials

Jean-Louis Auriault, Claude Boutin

Long wavelength inner-resonance cut-off frequencies in elastic composite materials

J.-L. Auriault [a,*], C. Boutin [b]

[a] 3S-R, Université Joseph Fourier, Institut National Polytechnique de Grenoble, CNRS, Domaine Universitaire, BP 53, 38041 Grenoble Cedex, France
[b] Université de Lyon, Ecole Nationale des Travaux Publics de l'Etat, LGM/DGCB CNRS 3237 Rue Maurice Audin, 69518 Vaulx-en-Velin, France

ABSTRACT

We revisit an ancient paper (Auriault and Bonnet, 1985) which points out the existence of cut-off frequencies for long acoustic wavelength in high-contrast elastic composite materials, i.e. when the wavelength is large with respect to the characteristic heterogeneity length. The separation of scales enables the use of the method of multiple scale expansions for periodic structures, a powerful upscaling technique from the heterogeneity scale to the wavelength scale. However, the results remain valid for non-periodic composite materials which show a Representative Elementary Volume (REV). The paper extends the previous investigations to three-component composite materials made of hard inclusions, coated with a soft material, both of arbitrary geometry, and embedded in a connected stiff material. The equivalent macroscopic models are rigorously established as well as their domains of validity. Provided that the stiffness contrast within the soft and the connected stiff materials is of the order of the squared separation of scales parameter, it is demonstrated (i) that the propagation of long wave may coincide with the resonance frequencies of the hard inclusions/soft material system and (ii) that the macroscopic model presents a series of cut-off frequencies given by an eigenvalue problem for the resonating domain in the cell. These results are illustrated in the case of stratified composites and the possible microstructures of heterogeneous media in which the inner dynamics phenomena may occur are discussed.

1. Introduction

This paper is devoted to the dynamics of elastic composite materials made of highly contrasted constituents. The contrast between the mechanical properties of the two or three constituents and the respective connectedness will be defined later. The composite material is either periodic or presenting a Representative Elementary Volume (REV) of characteristic size l. We are interested in wave propagation with a long wave-length Λ which is much larger than the size l of the period or of the REV. Let $L = \Lambda/2\pi$ be the macroscopic characteristic length of the excitation. The presence of the small parameter $\varepsilon = 2\pi l/\Lambda = l/L \ll 1$ enables us to use the homogenization method (Bensoussan et al., 1978; Sanchez-Palencia, 1980; Auriault et al., 2009), to investigate, by means of multiple scale expansions, an eventual equivalent macroscopic material.

Let us underline that this rigorous homogenization method procures some decisive advantages that will be exploited in the sequel: (1) avoiding prerequisites at macroscopic scale: the macroscopic equivalent description is obtained from the heterogeneity scale description plus the condition of separation of scales, only; (2) modeling finite size macroscopic samples and phenomena with finite macroscopic characteristic lengths ($\varepsilon \neq 0$); (3) modeling macroscopically non-homogeneous media or phenomena; (4) determining whether the system medium + phenomena is homogenizable or not, i.e., whether or not a continuous equivalent macroscopic description exists; (5) providing the domains of validity of the macroscopic models; note also the potential – not used in this study – for (6) modeling problems with several separations of scales by the introduction of several separation of scales parameters and for (7) modeling several simultaneous phenomena.

Moreover, when a separation of scales exists, i.e. for long wavelengths, periodic materials and non-periodic materials with REV show macroscopic behavior of the same nature (Auriault, 1991, 2011) (however, the solution is not reducible to a well-defined problem on a periodic cell in the case of a non-periodic medium). Therefore, we will assume the composite material as periodic without loss of generality. Of course, periodic and non-periodic media behave in a very different way when wavelengths become of the order of magnitude of the period or the REV. Note that the condition of scale separation is satisfied in a limited frequency range that excludes the cut-off frequencies resulting from diffraction phenomena at high frequency in periodic elastic composites. The whole paper focuses on the frequency range that respects the long wavelength condition.

The macroscopic behavior of high-contrast two-constituent elastic composite materials was rigorously investigated in Auriault and Bonnet (1985) (see Auriault, 1994 for an English version) by

* Corresponding author. Tel.: +33 4 76 82 70 77, Fax: +33 4 76 82 70 43.
E-mail address: Jean-Louis.Auriault@hmg.inpg.fr (J.-L. Auriault).

using the homogenization method. It was shown that when the high-rigidity solid is connected, and when both stiffness and wave celerity contrasts of the constituents are $\mathcal{O}(\varepsilon^2)$, the propagation of long waves induces local resonance within the soft medium. This phenomenon leads to a frequency dependent effective tensorial density different from the real scalar density. At macroscopic scale, the description generalizes the Newtonian mechanics by introducing non local effect in time. In this situation, waves become dispersive and frequency band-gaps occur around a series of local resonance frequencies (in the limit of the long wavelength assumption). To clearly distinguish this phenomena from the cut-off frequencies induced by diffraction in periodic lattices, we use the term of inner-resonance cut-off frequency. Such materials, named nowadays as "metamaterials", are of prime interest for wave insulation or filtering.

More recently, the subject has received new interest. The theoretical mathematical study of the local elastic resonance mechanism has been investigated in the work of Zhikov (2000) and Ávila et al. (2005) (for fiber composites) followed in the same line by Babych et al. (2008) and Smyshlyaev (2009), providing results on the convergence of the asymptotic approach. For reticulated structures experiencing global vibrations, inner dynamic phenomena due to local resonance in bending have also been evidenced (Boutin et al., 2010). Experiments on contrasted composites made of epoxy matrix–duraluminium cylinders (Vasseur et al., 1998) or made of epoxy matrix- embedding lead spheres coated by silicon rubber (Liu et al., 2000, 2005; She et al., 2003) clearly demonstrate the existence of band gaps related to local resonance. The reader is referred to Milton and Willis (2007), where such modifications of the Newton's second law are investigated and where different physical contexts about metamaterials are given.

The aim of this paper is to investigate the possible microstructures of heterogeneous media in which the propagation of long wave coincides with the resonance frequency (ies) of a (or several) component of the period. In Section 2, we recall and comment the main results of Auriault and Bonnet (1985) for bi-composites. In Section 3, the equivalent macroscopic models of three-component materials (hard inclusion coated with a soft material within a connected stiff material) are established for arbitrary geometries. The macroscopic model is similar to the two-constituent model and presents a series of inner-resonance cut-off frequencies on the condition that the stiffness contrast within soft and stiff material is $\mathcal{O}(\varepsilon^2)$. Further, when the soft medium is of smaller density than the other components by an order $\varepsilon^q, q \geqslant 1$, the coated hard inclusion behaves as a 3D spring-mass system, and the inner-resonance cut-off frequencies are related to the few actual degrees of freedom. Finally, these results are illustrated and discussed in the case of stratified composites by considering macroscopic P waves which propagate and are polarized in the plane layer direction. The stiff layers undergo an in plane compression vibration whereas the soft layers experience a shear forced vibration which propagate perpendicularly to the layers.

2. Composite made of connected high-rigidity solid and soft medium

As in Auriault and Bonnet (1985) and Smyshlyaev (2009), we consider a two component Ω-periodic composite made of a connected high-rigidity solid s and of a soft medium m which is connected or not connected. However, the analysis remains valid provided that the stiff component is connected in the wave propagation direction, see Section 4 where analytical results are presented. For the sake of simplicity, when non connected, the soft medium shows a single inclusion in the period, as in Fig. 1. Media s and m, which for simplicity are assumed as homogeneous, with

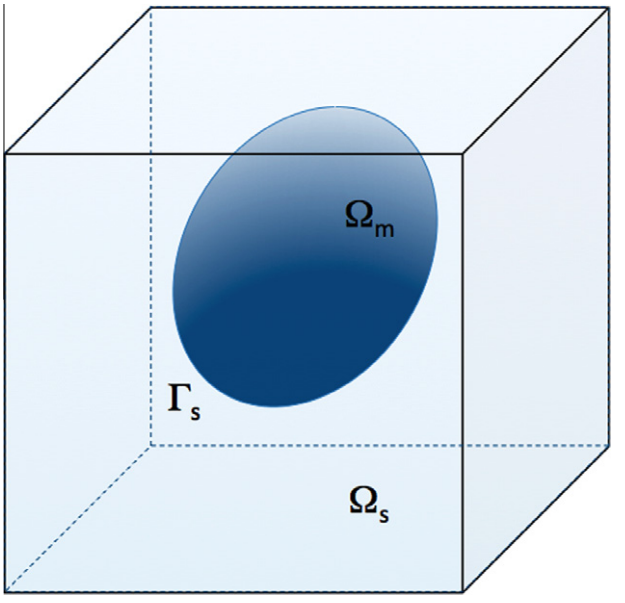

Fig. 1. A period of a composite material with connected high-rigidity solid s and soft inclusion m.

uniform elastic tensors $\mathbf{a}_s$ and $\mathbf{a}_m$ and with constant densities ρ_s and ρ_m, occupy the domains Ω_s and Ω_m, respectively. The concentration of constituents are respectively $c_i = |\Omega_i|/|\Omega|$, i = s, m. The interface between Ω_m and Ω_s is denoted Γ_s.

2.1. Heterogeneity scale description and estimations

Under an acoustic perturbation, the medium satisfies the Navier equation in Ω_s and Ω_m, with standard conditions on the interface Γ_s, i.e. the continuity of normal stress vector and of displacement:

$$\mathrm{div}_X(\boldsymbol{\sigma}) = \rho \frac{\partial^2 \mathbf{u}}{\partial t^2}, \tag{1}$$

$$\boldsymbol{\sigma} = \mathbf{a} : \mathbf{e}_X(\mathbf{u}) \quad \text{within } \Omega \tag{2}$$

and

$$(\boldsymbol{\sigma}_s - \boldsymbol{\sigma}_m) \cdot \mathbf{n}_s = 0, \tag{3}$$

$$\mathbf{u}_s - \mathbf{u}_m = 0 \quad \text{over } \Gamma_s. \tag{4}$$

In the above equations, $\mathbf{X} = (X_1, X_2, X_3)$ is the physical space variable, $\boldsymbol{\sigma}$ is the stress, $\mathbf{e}$ is the deformation and $\mathbf{u}$ is the displacement. Variables indexed by m or s refer respectively to medium m or s. $\mathbf{n}_s$ is the unit normal vector exterior to Ω_s. Let us make dimensionless the above equations by using l as the characteristic length. We consider low frequencies ω such that the corresponding wavelength Λ_s in medium s is large with respect to l. We have

$$\frac{\Lambda_s}{2\pi} = \frac{1}{\omega}\sqrt{\frac{|\,\mathbf{a}_s\,|}{\rho_s}} \quad \text{and} \quad L = \mathcal{O}\left(\frac{\Lambda_s}{2\pi}\right),$$

which yields

$$\rho_s \omega^2 = \varepsilon^2 \frac{|\,\mathbf{a}_s\,|}{l^2}.$$

Therefore, it comes

$$\mathcal{P}_l = \frac{\left|\rho_s \frac{\partial^2 \mathbf{u}_s}{\partial t^2}\right|}{|\,\mathrm{div}_X(\boldsymbol{\sigma}_s)\,|} = \mathcal{O}\left(\frac{\rho_s \omega^2 l^2}{|\,\mathbf{a}_s\,|}\right) = \mathcal{O}(\varepsilon^2),$$

where the dimensionless number $\mathcal{P}_l$ is evaluated by using the characteristic length l. We consider a high contrast between the wave

celerities of the stiff medium and that of the soft medium, of the order ε:

$$\frac{C_m}{C_s} = \sqrt{\mathcal{Q}} = \mathcal{O}(\varepsilon), \quad \mathcal{Q} = \frac{|\,\mathbf{a}_m\,|\,\rho_s}{|\,\mathbf{a}_s\,|\,\rho_m} = \mathcal{O}(\varepsilon^2).$$

This implies that the wavelength in medium m is of the order of magnitude of l

$$\frac{\Lambda_m}{2\pi} = \frac{1}{\omega}\sqrt{\frac{|\,\mathbf{a}_m\,|}{\rho_m}} = \mathcal{O}(l).$$

Therefore, the investigated situation involves two interacting dynamic phenomena, one at macro-scale carried trough the stiff medium, and one at micro-scale occurring in the soft medium.

In the sequel, the densities are assumed to be of the same order of magnitude and consequently

$$\frac{\rho_s}{\rho_m} = \mathcal{O}(1); \quad \frac{|\,\mathbf{a}_m\,|}{|\,\mathbf{a}_s\,|} = \mathcal{O}(\varepsilon^2).$$

It can be deduced from the previous assumptions that the displacements in the solid and the matrix are of similar order of magnitude

$$\mathbf{u}_s = \mathcal{O}(\mathbf{u}_m).$$

Finally, the dimensionless equations at the heterogeneity scale, that describe the wave propagation at constant angular frequency ω take the form (the time dependance $\exp(i\omega t)$ simplifies by linearity and is systematically omitted)

$$\mathrm{div}_y(\mathbf{a}_s : \mathbf{e}_y(\mathbf{u}_s)) = -\varepsilon^2\omega^2\rho_s\mathbf{u}_s \quad \text{within } \Omega_s, \tag{5}$$

$$\mathrm{div}_y(\mathbf{a}_m : \mathbf{e}_y(\mathbf{u}_m)) = -\omega^2\rho_m\mathbf{u}_m \quad \text{within } \Omega_m \tag{6}$$

and

$$(\boldsymbol{\sigma}_s - \varepsilon^2\boldsymbol{\sigma}_m)\cdot\mathbf{n}_s = 0, \tag{7}$$

$$\mathbf{u}_s - \mathbf{u}_m = 0 \quad \text{over } \Gamma_s, \tag{8}$$

where $\mathbf{y} = \mathbf{X}/l$. To lighten the writing, notations for the other quantities are kept identical whatever in dimensionless or physical form.

2.2. Homogenization process

The homogenization process consists in introducing two dimensionless space variables, $\mathbf{y} = \mathbf{X}/l$ and $\mathbf{x} = \mathbf{X}/L$ with $\mathbf{x} = \varepsilon\mathbf{y}$, and to look for the displacement in the form of the following asymptotic expansion

$$\mathbf{u} = \mathbf{u}^{(0)}(\mathbf{x},\mathbf{y}) + \varepsilon\mathbf{u}^{(1)}(\mathbf{x},\mathbf{y}) + \varepsilon^2\mathbf{u}^{(2)}(\mathbf{x},\mathbf{y}) + \cdots, \tag{9}$$

where the $\mathbf{u}^{(i)}(\mathbf{x},\mathbf{y})$ are $\mathbf{y}$-periodic functions. Introducing expansion (9) into the local dimensionless set (5)–(8) and equating like powers of ε yield successive boundary value problems to be investigated on the period. Let us briefly recall the results developed in Auriault and Bonnet (1985) and Auriault (1994) (the periodicity conditions systematically apply for media occupying connected domains and are not explicitly mentioned in the sequel).

2.2.1. Resolution in the stiff and connected media

Eqs. (5) and (7) give at the first order

$$\mathrm{div}_y(\mathbf{a}_s : \mathbf{e}_y(\mathbf{u}_s^{(0)})) = 0 \quad \text{within } \Omega_s,$$

$$(\mathbf{a}_s : \mathbf{e}_y(\mathbf{u}_s^{(0)}))\cdot\mathbf{n}_s = 0 \quad \text{over } \Gamma_s.$$

Therefore, the movement of medium s is a periodic rigid motion at the first order of magnitude. Because medium s is connected, this rigid motion reduces to a translation at the heterogeneity scale

$$\mathbf{u}_s^{(0)} = \mathbf{U}_s^{(0)}(\mathbf{x}). \tag{10}$$

– At the following order, Eqs. (5) and (7) yield

$$\mathrm{div}_y(\mathbf{a}_s : (\mathbf{e}_y(\mathbf{u}_s^{(1)}) + \mathbf{e}_x(\mathbf{U}_s^{(0)}))) = 0 \quad \text{within } \Omega_s,$$

$$(\mathbf{a}_s : \mathbf{e}_y(\mathbf{u}_s^{(1)}) + \mathbf{e}_x(\mathbf{U}_s^{(0)}))\cdot\mathbf{n}_s = 0 \quad \text{over } \Gamma_s.$$

We obtain classically the solution of this *elasto-static* problem in the form

$$\mathbf{u}_s^{(1)} = \boldsymbol{\chi}_s(\mathbf{y}) : \mathbf{e}_x(\mathbf{U}_s^{(0)}) + \mathbf{U}_s^{(1)}(\mathbf{x}), \tag{11}$$

where the tensor $\boldsymbol{\chi}_s(\mathbf{y})$ depends only on the elastic properties and on the geometry of medium s.– At the third order, Eqs. (5) and (7) write

$$\mathrm{div}_y(\mathbf{a}_s : (\mathbf{e}_y(\mathbf{u}_s^{(2)}) + \mathbf{e}_x(\mathbf{u}_s^{(1)}))) + \mathrm{div}_x(\mathbf{a}_s : (\mathbf{e}_y(\mathbf{u}_s^{(1)}) + \mathbf{e}_x(\mathbf{U}_s^{(0)}))) = -\omega^2\rho_s\mathbf{U}_s^{(0)},$$

within Ω_s and

$$(\mathbf{a}_s : \mathbf{e}_y(\mathbf{u}_s^{(2)}) + \mathbf{e}_x(\mathbf{u}_s^{(1)}))\cdot\mathbf{n}_s = (\mathbf{a}_m : \mathbf{e}_y(\mathbf{u}_m^{(0)}))\cdot\mathbf{n}_s \quad \text{over } \Gamma_s.$$

After integration over Ω_s, the use of the divergence theorem and the periodicity condition, it comes the following macroscopic relation (i.e. independent on $\mathbf{y}$)

$$\mathrm{div}_x(\mathbf{A}_s^{eff} : \mathbf{e}_x(\mathbf{U}_s^{(0)})) = -\omega^2 c_s\rho_s\mathbf{U}_s^{(0)} - \frac{1}{|\,\Omega\,|}\int_{\Gamma_s}(\mathbf{a}_m : \mathbf{e}_y(\mathbf{u}_m^{(0)}))\cdot\mathbf{n}_s d\Gamma, \tag{12}$$

where $\mathbf{A}_s^{eff}$ is the effective elastic tensor of constituent s (i.e. as in the absence of constituent m)

$$\mathbf{A}_s^{eff} = \langle\mathbf{a}_s : \mathbf{e}_y(\boldsymbol{\chi}_s) + \mathbf{a}_s\rangle_s,$$

with the notations used herein and in the following

$$\langle\cdot\rangle_n = \frac{1}{|\,\Omega\,|}\int_{\Omega_n}\cdot\,d\Omega, \quad n = s,m, \quad \text{and} \quad \langle\cdot\rangle = \frac{1}{|\,\Omega\,|}\int_{\Omega}\cdot\,d\Omega$$

2.2.2. Resolution in the soft medium

The first order displacement in medium m is given by Eqs. (6) and (8) at order 0

$$\mathrm{div}_y(\mathbf{a}_m : \mathbf{e}_y(\mathbf{u}_m^{(0)})) = -\omega^2\rho_m\mathbf{u}_m^{(0)} \quad \text{within } \Omega_m, \tag{13}$$

$$\mathbf{u}_m^{(0)} = \mathbf{U}_s^{(0)}(\mathbf{x}) \quad \text{over } \Gamma_s. \tag{14}$$

To study this *elasto-dynamic* problem with Dirichlet condition, we put

$$\mathbf{u}_m^{(0)} = \mathbf{v} + \mathbf{U}_s^{(0)}.$$

The boundary value problem becomes

$$\mathrm{div}_y(\mathbf{a}_m : \mathbf{e}_y(\mathbf{v})) = -\omega^2\rho_m(\mathbf{v} + \mathbf{U}_s^{(0)}) \quad \text{within } \Omega_m, \tag{15}$$

$$\mathbf{v} = 0 \quad \text{over } \Gamma_s. \tag{16}$$

Let us introduce the eigenvalue problem associated with the operator in the left hand member in (15), with the boundary conditions (16)

$$\mathrm{div}_y(\mathbf{a}_m : \mathbf{e}_y(\boldsymbol{\phi})) = -\lambda\boldsymbol{\phi} \quad \text{within } \Omega_m,$$

$$\boldsymbol{\phi} = 0 \quad \text{over } \Gamma_s.$$

The spectrum is discrete and positive (Courant and Hilbert, 1970)

$$0 \leqslant \lambda_1 \leqslant \lambda_2 \leqslant \lambda_3 \leqslant \cdots$$

each eigenvalue λ_i being associated to a vectorial eigenfunction ${}^i\boldsymbol{\phi}$. The series $\{{}^i\boldsymbol{\phi}\}$ constitute an orthogonal basis on which $\mathbf{v}$ can be decomposed. To this aim, note first that from the divergence theorem, the periodicity condition and the zero motion condition over Γ_s we have

$$\int_{\Omega_m}\mathrm{div}_y(\mathbf{a}_m : \mathbf{e}_y({}^i\boldsymbol{\phi}))\cdot\mathbf{v}\,d\Omega = \int_{\Omega_m}\mathrm{div}_y(\mathbf{a}_m : \mathbf{e}_y(\mathbf{v}))\cdot{}^i\boldsymbol{\phi}\,d\Omega.$$

This equality, re-expressed with the balance equation of both field $\mathbf{v}$ and ${}^i\boldsymbol{\phi}$, reads (no summation on i on left hand side)

$$\lambda_i \int_{\Omega_m} {}^i\boldsymbol{\phi}.\mathbf{v}\mathrm{d}\Omega = \omega^2 \rho_m \int_{\Omega_m} (\mathbf{v} + \mathbf{U}_s^{(0)}).{}^i\boldsymbol{\phi}\mathrm{d}\Omega$$

Then, the orthogonality of the eigenfunctions enables us to write $\mathbf{v}$ in the form

$$\mathbf{v} = \mathbf{u}_m^{(0)} - \mathbf{U}_s^{(0)} = \sum_{i=1}^{\infty} \frac{\mathbf{U}_s^{(0)}.\langle {}^i\boldsymbol{\phi}\rangle_m}{\langle \|{}^i\boldsymbol{\phi}\|^2\rangle_m} \frac{{}^i\boldsymbol{\phi}}{\frac{\lambda_i}{\omega^2\rho_m} - 1} = \boldsymbol{\alpha}(\mathbf{y},\omega)\cdot\mathbf{U}_s^{(0)}. \tag{17}$$

Therefore, a solution of (15) and (16) exists when

$$\omega \neq \omega_i = \left(\frac{\lambda_i}{\rho_m}\right)^{1/2}, \quad i = 1,2,\ldots$$

If $\omega = \omega_i$, the solution exists when the corresponding vectorial eigenfunction ${}^i\boldsymbol{\phi}$ is orthogonal to $\mathbf{U}^{(0)}$ over Ω_m, i.e. if $\langle {}^i\boldsymbol{\phi}\rangle_m = 0$. When this condition is not met, $\mathbf{v}$ is not bounded in the vicinity of ω_i. Its components change their sign if λ_i is a single eigenvalue. Consequently, the second order tensor $\boldsymbol{\alpha}$ is possibly not bounded and changing its sign at $\omega = \omega_i$.

2.2.3. Equivalent macroscopic description

We can now calculate the integral in the right hand member of (12). It comes with (13) and (17)

$$\int_{\Gamma_s} (\mathbf{a}_m : \mathbf{e}_y(\mathbf{u}_m^{(0)}))\cdot\mathbf{n}_s\mathrm{d}\Gamma = -\int_{\Omega_m} \mathrm{div}_y(\mathbf{a}_m : \mathbf{e}_y(\mathbf{u}_m^{(0)}))\mathrm{d}\Omega$$
$$= \int_{\Omega_m} \omega^2\rho_m\mathbf{u}_m^{(0)}\mathrm{d}\Omega = \int_{\Omega_m} \omega^2\rho_m(\mathbf{I}+\boldsymbol{\alpha})\cdot\mathbf{U}_s^{(0)}\mathrm{d}\Omega.$$

Finally, we obtain the equivalent macroscopic behavior of the composite material in the form

$$\mathrm{div}_x(\mathbf{A}_s^{eff} : \mathbf{e}_x(\mathbf{U}_s^{(0)})) = -\omega^2\boldsymbol{\rho}^{eff}(\omega)\mathbf{U}_s^{(0)}, \tag{18}$$

where

$$\boldsymbol{\rho}^{eff}(\omega) = \langle\rho\rangle\mathbf{I} + \rho_m\langle\boldsymbol{\alpha}\rangle_m; \quad \langle\boldsymbol{\alpha}\rangle_m = \sum_{i=1}^{\infty} \frac{\langle {}^i\boldsymbol{\phi}\rangle_m \otimes \langle {}^i\boldsymbol{\phi}\rangle_m}{\langle \|{}^i\boldsymbol{\phi}\|^2\rangle_m} \frac{1}{\left(\frac{\omega_i}{\omega}\right)^2 - 1}.$$

The effective density $\boldsymbol{\rho}^{eff}$ is of tensorial character and depends on the frequency. Note that the tensor $\langle\boldsymbol{\alpha}\rangle_m$ depends on the frequency and on the elastic properties, the density and the geometry of medium m only.

Let us return to dimensional quantities. The macroscopic description is obtained within an approximation $\mathcal{O}(\varepsilon)$

$$\mathrm{div}_X(\mathbf{A}_s^{eff} : \mathbf{e}_X(\mathbf{u}_s)) = -\omega^2\boldsymbol{\rho}^{eff}(\omega)\cdot\mathbf{u}_s + \mathcal{O}(\varepsilon). \tag{19}$$

$\boldsymbol{\rho}^{eff}$, as $\langle\boldsymbol{\alpha}\rangle_m$, is generally not bounded and changes its sign in the vicinity of ω_i. These latter eigenfrequencies ω_i correspond to the resonances of constituent m submitted to fixed boundary condition over Γ_s (and periodic condition if Ω_m is connected and thus intersects the boundary of the period). The macroscopic medium is dispersive and the wave celerity and wave length are of the order of

$$C^{eff} = \mathcal{O}\left(\sqrt{\frac{|\mathbf{A}_s^{eff}|}{|\boldsymbol{\rho}^{eff}(\omega)|}}\right); \quad \Lambda^{eff} = \mathcal{O}(C^{eff}/\omega).$$

Let us consider, for simplicity, a composite with macroscopic elastic and inertial isotropy. The wave number $k = \omega/C^{eff}$ is schematically shown in Fig. 2 as a function of the pulsation ω. Hatched areas correspond to negative densities $\boldsymbol{\rho}^{eff}$, i.e., to stopping bands. On an other hand, as $\boldsymbol{\rho}^{eff}$ increases, the wavelength decreases. The separation of scales becomes worse, a macroscopic description no longer exists and diffraction occurs. This situation is attained when $\Lambda^{eff} = \mathcal{O}(l)$, which means

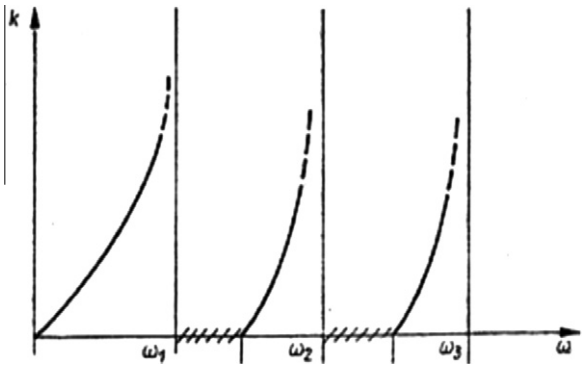

Fig. 2. Wave number versus angular frequency (from Auriault and Bonnet, 1985). Hatched areas: stopping bands. Dashed lines: non homogenizable areas. Solid lines: passing bands.

$$\mathcal{O}(|\boldsymbol{\rho}^{eff}(\omega)|) = \rho_m\frac{|\mathbf{A}_s^{eff}|}{|\mathbf{a}_m|}.$$

According to the singularities of $|\boldsymbol{\rho}^{eff}(\omega)|$ around ω_k, the "exclusion" band frequency $\Delta\omega_k$ is of the order of:

$$2\frac{\Delta\omega_k}{\omega_k} = \mathcal{O}\left(\left(\frac{|\mathbf{A}_s^{eff}|}{|\mathbf{a}_m|} - \frac{\langle\rho\rangle}{\rho_m}\right)^{-1}\right) = \mathcal{O}\left(\frac{|\mathbf{a}_m|}{|\mathbf{a}_s|}\right).$$

This is shown by dashed lines in Fig. 2. In these regions, the separation of scales becomes poor or inexistent. When the separation of scales is poor, diffraction occurs that can be investigated by analyzing the correctors Boutin and Auriault, 1993. The values of ω corresponding to solid lines belong to passing bands. The wave filtering role of the present composite material occurs for long wavelengths (i.e. low frequencies). It is due to resonance effects. An analytical example of wave propagation through bi-composite layered media in the layer direction is given in Auriault and Bonnet (1985) (see examples treated in Section 4).

2.3. Damping effect

We investigate here the influence of a slight damping by considering a viscoelastic behavior of the soft constituent. Hence $\mathbf{a}_m$, in the Fourier space is replaced by a complex viscoelastic tensor $\mathbf{a}_m + i\mathbf{b}_m$. The eigenvalue problem reads now

$$\mathrm{div}_y((\mathbf{a}_m + i\mathbf{b}_m) : \mathbf{e}_y(\boldsymbol{\phi}^*)) = -\lambda^*\boldsymbol{\phi}^* \quad \text{within } \Omega_m,$$
$$\boldsymbol{\phi}^* = 0 \quad \text{over } \Gamma_s.$$

When assuming $|\mathbf{b}_m| \ll |\mathbf{a}_m|$, the viscoelastic eigenvalues $\{\lambda_i^*\}$ and the eigenvectors $\{{}^i\boldsymbol{\phi}^*\}$ are deduced from the elastic case through an asymptotic procedure. In this aim, let us write

$$\lambda^* = \lambda + \widetilde{\lambda} + \cdots; \quad \boldsymbol{\phi}^* = \boldsymbol{\phi} + \widetilde{\boldsymbol{\phi}} + \cdots$$

The equation governing the first corrector is:

$$\mathrm{div}_y(\mathbf{a}_m : \mathbf{e}_y(\widetilde{\boldsymbol{\phi}})) + i\mathrm{div}_y(\mathbf{b}_m : \mathbf{e}_y(\boldsymbol{\phi})) = -(\widetilde{\lambda}\boldsymbol{\phi} + \lambda\widetilde{\boldsymbol{\phi}}) \quad \text{within } \Omega_m,$$
$$\widetilde{\boldsymbol{\phi}} = 0 \quad \text{over } \Gamma_s.$$

Focusing on the kth elastic mode and its viscoelastic corrector, we deduce from the usual integral transformation and the boundary conditions

$$\int_{\Omega_m} \mathrm{div}_y(\mathbf{a}_m : \mathbf{e}_y({}^k\boldsymbol{\phi}))\cdot{}^k\widetilde{\boldsymbol{\phi}}\mathrm{d}\Omega = \int_{\Omega_m} \mathrm{div}_y(\mathbf{a}_m : \mathbf{e}_y({}^k\widetilde{\boldsymbol{\phi}}))\cdot{}^k\boldsymbol{\phi}\mathrm{d}\Omega$$

and, with the balance equation of both fields, we derive (no summation on k)

$$\widetilde{\lambda}_k = -i\frac{\langle \mathbf{e}_y({}^k\boldsymbol{\phi}) : \mathbf{b}_m : \mathbf{e}_y({}^k\boldsymbol{\phi})\rangle_m}{\langle \|{}^k\boldsymbol{\phi}\|^2\rangle_m} = -i\lambda_k\xi_k; \quad \xi_k \ll 1.$$

This result enables to determine ${}^k\widetilde{\boldsymbol{\phi}}$ from the equation governing the first corrector at the heterogeneity scale (let us simply mention that ${}^k\widetilde{\boldsymbol{\phi}}$ is purely imaginary and orthogonal to ${}^k\boldsymbol{\phi}$).

Finally, the effective density becomes complex-valued

$$\boldsymbol{\rho}^{eff*}(\omega) = \langle\rho\rangle\mathbf{I} + \rho_m\langle\boldsymbol{\alpha}^*\rangle_m;$$
$$\langle\boldsymbol{\alpha}^*\rangle_m = \sum_{i=1}^{\infty} \frac{\langle {}^k\boldsymbol{\phi}^*\rangle_m \otimes \langle {}^k\boldsymbol{\phi}^*\rangle_m}{\langle \|{}^k\boldsymbol{\phi}^*\|^2\rangle_m} \frac{1}{\frac{\lambda_k^*}{\omega^2\rho_m} - 1}$$

and we obtain in the vicinity of ω_k

$$\frac{1}{\frac{\lambda_k^*}{\omega^2\rho_m} - 1} \sim i\xi_k^{-1}; \quad \boldsymbol{\rho}^{eff*}(\omega_k) \sim \langle\rho\rangle\mathbf{I} + i\rho_m\xi_k^{-1}\boldsymbol{\beta}_k; \quad \boldsymbol{\beta}_k = \mathcal{O}(1).$$

Therefore, the consequence of a slight viscoelastic effect in medium m is a damping of the resonance phenomena, that results in the regularization of the singularities of the effective density: $|\,\boldsymbol{\rho}^{eff*}(\omega)\,|$ is bounded and presents a continuous phase inversion around the eigenfrequencies. Note that replacing the stiff elastic medium by a viscoelastic medium would modify $\mathbf{A}_s^{eff}$ without changing $\boldsymbol{\rho}^{eff}$.

2.4. Soft inclusion and different celerity ratio

In this section we consider moderate and extremely high celerity contrast between the soft and the connected stiff media. We have, as above

$$L = \mathcal{O}\left(\frac{\Lambda_s}{2\pi}\right) = \mathcal{O}\left(\frac{1}{\omega}\sqrt{\frac{|\,\mathbf{a}_s\,|}{\rho_s}}\right) \quad \text{hence,} \quad \rho_s\omega^2 = \varepsilon^2\frac{|\,\mathbf{a}_s\,|}{l^2}.$$

The contrast between the wave celerity of the stiff solid and that of the soft medium is now

$$\mathcal{Q} = \frac{|\,\mathbf{a}_m\,|\,\rho_s}{|\,\mathbf{a}_s\,|\,\rho_m} = \mathcal{O}(\varepsilon^p), \quad p = 1 \text{ or } p \geqslant 3.$$

Consequently, the order of magnitude of the wavelength in medium m reads

$$\frac{\Lambda_m}{2\pi} = \frac{1}{\omega}\sqrt{\frac{|\,\mathbf{a}_m\,|}{\rho_m}} = \mathcal{O}(l\varepsilon^{p/2-1}).$$

It is either significantly higher ($p = 1$) or lower ($p \geqslant 3$) than the heterogeneity size. As above, densities are assumed of the same order of magnitude and, consequently, the contrast of the elastic properties are either moderate ($p = 1$) or extremely high ($p \geqslant 3$)

$$\frac{|\,\mathbf{a}_m\,|}{|\,\mathbf{a}_s\,|} = \mathcal{O}(\varepsilon^p), \quad p = 1 \text{ or } p \geqslant 3.$$

Following the same route as in Section 2.2 yields the equivalent macroscopic models.

When $p = 1$, the dimensionless equations that describe the wave propagation at constant frequency are now in the form

$$\mathrm{div}_y(\mathbf{a}_s : \mathbf{e}_y(\mathbf{u}_s)) = -\varepsilon^2\omega^2\rho_s\mathbf{u}_s \quad \text{within } \Omega_s,$$
$$\mathrm{div}_y(\mathbf{a}_m : \mathbf{e}_y(\mathbf{u}_m)) = -\varepsilon\omega^2\rho_m\mathbf{u}_m \quad \text{within } \Omega_m$$

and

$$(\boldsymbol{\sigma}_s - \varepsilon\boldsymbol{\sigma}_m)\cdot\mathbf{n}_s = 0,$$
$$\mathbf{u}_s - \mathbf{u}_m = 0 \quad \text{over } \Gamma_s.$$

The difference with the previous case is that medium m is in a quasi-static state at the leading order and therefore it moves identically to the stiff medium, i.e. $\mathbf{u}_m^{(0)} = \mathbf{U}_s^{(0)}$. We thus obtain the following macroscopic description which corresponds to the classical description of an elastic composite (with a soft component)

$$\mathrm{div}_X(\mathbf{A}_s^{eff} : \mathbf{e}_X(\mathbf{u}_s)) = -\omega^2\langle\rho\rangle\mathbf{u}_s + \mathcal{O}(\varepsilon),$$

where, as usual, the effective density is independent on the frequency and is given by the scalar mean density $\langle\rho\rangle = c_s\rho_s + c_m\rho_m$. In this case, inner-resonance cut-off frequencies are absent.

When $p \geqslant 3$, the dimensionless equations in medium s read

$$\mathrm{div}_y(\mathbf{a}_s : \mathbf{e}_y(\mathbf{u}_s)) = -\varepsilon^2\omega^2\rho_s\mathbf{u}_s \quad \text{within } \Omega_s,$$
$$(\boldsymbol{\sigma}_s - \varepsilon^p\boldsymbol{\sigma}_m)\cdot\mathbf{n}_s = 0, \quad \text{over } \Gamma_s.$$

This set enables to derive the equivalent macroscopic model at the leading order, which corresponds to a medium constituted by constituent s only.

$$\mathrm{div}_X(\mathbf{A}_s^{eff} : \mathbf{e}_X(\mathbf{u}_s)) = -\omega^2 c_s\rho_s\mathbf{u}_s + \mathcal{O}(\varepsilon),$$

At the leading order, the extremely soft medium m neither contributes to the overall elastic properties (which are then similar to those of the stiff media with empty inclusions) nor to inertia (despite the fact that its density is of the same order as that of medium s). The reason lies in the fact that the large number of very small wave lengths occurring in the soft medium domain leads in average to a negligible inertia. Hence, the effective density ρ_s^{eff}, which is given by $c_s\rho_s$, does not depend on the frequency. Cut-off frequencies are absent, but the high dynamics within medium m results in an apparent lightening of the medium.

2.5. Rigid inclusion embedded in a softer material

To be thorough, let us briefly consider the converse situation of hard inclusions s embedded in a soft matrix m when Ω_m is connected and Ω_s is not connected (in this section only). An equivalent macroscopic model exists iff a separation of scales is present. In this configuration, the macro-dynamics is governed by the soft matrix and therefore

$$L = \mathcal{O}\left(\frac{\Lambda_m}{2\pi}\right),$$

which yields

$$\frac{1}{\omega}\sqrt{\frac{|\,\mathbf{a}_m\,|}{\rho_m}} = \varepsilon^{-1}l, \quad \text{thus} \quad \rho_m\omega^2 = \varepsilon^2\frac{|\,\mathbf{a}_m\,|}{l^2}.$$

The elastic wave celerity contrast is estimated as

$$\mathcal{Q} = \frac{|\,\mathbf{a}_m\,|\,\rho_s}{|\,\mathbf{a}_s\,|\,\rho_m} = \mathcal{O}(\varepsilon^p), \quad p \geqslant 1.$$

Consequently, the wavelengths in both constituents are at least one order higher than the heterogeneity size

$$\frac{\Lambda_m}{2\pi} = \mathcal{O}(\varepsilon^{-1}l); \quad \frac{\Lambda_s}{2\pi} = \frac{1}{\omega}\sqrt{\frac{|\,\mathbf{a}_s\,|}{\rho_s}} = \mathcal{O}(\varepsilon^{-1-p/2}l)$$

and therefore this macro-dynamics situation is expected not to introduce any inner dynamics phenomena.

The dimensionless equations that describe the wave propagation at constant frequency at the heterogeneity scales are now

$$\mathrm{div}_y(\mathbf{a}_s : \mathbf{e}_y(\mathbf{u}_s)) = -\varepsilon^{2+p}\omega^2\rho_s\mathbf{u}_s \quad \text{within } \Omega_s,$$
$$\mathrm{div}_y(\mathbf{a}_m : \mathbf{e}_y(\mathbf{u}_m)) = -\varepsilon^2\omega^2\rho_m\mathbf{u}_m \quad \text{within } \Omega_m$$

and

$$(\boldsymbol{\sigma}_s - \varepsilon^p\boldsymbol{\sigma}_m)\cdot\mathbf{n}_s = 0,$$
$$\mathbf{u}_s - \mathbf{u}_m = 0 \quad \text{over } \Gamma_s.$$

The homogenization process is that of the classical case of a composite material with rigid inclusions (Léné, 1978); it provides the equivalent macroscopic model

$$\mathrm{div}_X(\mathbf{A}^{eff} : \mathbf{e}_X(\mathbf{u})) = -\omega^2\langle\rho\rangle\mathbf{u} + \mathcal{O}(\varepsilon),$$

where $\mathbf{A}^{eff}$ is the effective elastic tensor of medium m in presence of rigid inclusions s, and the effective density is the scalar mean density (independent on ω). Obviously, in absence of inner dynamics, inner-resonance cut-off frequencies do not appear.

3. Three-component material

We now consider that, within the stiff connected solid, the soft medium m itself contains an un-connected inclusion of stiffer material r of boundary Γ_r, see Fig. 3. The composite material investigated in Liu et al. (2000, 2005) and Sheng et al. (2003) corresponds to the particular case where Γ_s and Γ_r are concentric spheres. In this section materials are assumed elastic. The study of visco-elastic constituents could be addressed in the same manner as for bi-composite, and the viscous dissipation would lead qualitatively to effects of the same nature.

3.1. Heterogeneity scale description and estimations

Under an acoustic perturbation, the three-component composite satisfies the following equations

$$\mathrm{div}_X(\boldsymbol{\sigma}) = \rho\frac{\partial^2\mathbf{u}}{\partial t^2}, \tag{20}$$

$$\boldsymbol{\sigma} = \mathbf{a} : \mathbf{e}_X(\mathbf{u}) \quad \text{within } \Omega. \tag{21}$$

The boundary conditions are

$$(\boldsymbol{\sigma}_s - \boldsymbol{\sigma}_m)\cdot\mathbf{n}_s = 0, \tag{22}$$

$$\mathbf{u}_s - \mathbf{u}_m = 0 \quad \text{over } \Gamma_s \tag{23}$$

and

$$(\boldsymbol{\sigma}_r - \boldsymbol{\sigma}_m)\cdot\mathbf{n}_r = 0, \tag{24}$$

$$\mathbf{u}_r - \mathbf{u}_m = 0 \quad \text{over } \Gamma_r. \tag{25}$$

We will also use the momentum and the moment of momentum balances of inclusion r

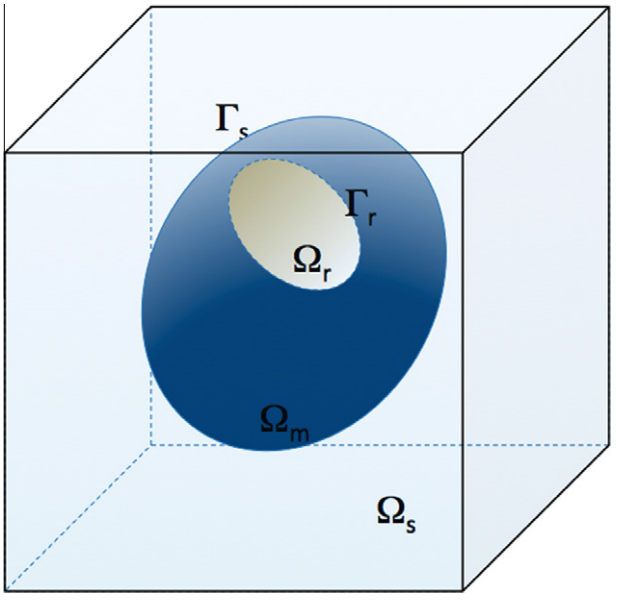

Fig. 3. Three-component material. The period is constituted by stiff connected solid m, and a soft medium m containing an un-connected inclusion of hard material r.

$$\int_{\Omega_r}\rho_r\omega^2\mathbf{u}_r d\Omega = -\int_{\Gamma_r}\boldsymbol{\sigma}_m\cdot\mathbf{n}_r\, d\Omega, \tag{26}$$

$$\int_{\Omega_r}\rho_r\omega^2\mathbf{X}\wedge\mathbf{u}_r d\Omega = -\int_{\Gamma_r}\mathbf{X}\wedge\boldsymbol{\sigma}_m\cdot\mathbf{n}_r d\Omega, \tag{27}$$

where the origin of the space variable $\mathbf{X}$ is at the center of mass of inclusion r and $\mathbf{n}_r$ is the unit normal vector exterior to medium r.

The relative orders of magnitude of the elastic wave celerities of media s and m are taken as above:

$$\frac{|\,\mathbf{a}_m\,|\,\rho_s}{|\,\mathbf{a}_s\,|\,\rho_m} = \mathcal{O}(\varepsilon^2),$$

while the wave celerity of inclusion r is assumed higher than in medium m,

$$\frac{|\,\mathbf{a}_m\,|\,\rho_r}{|\,\mathbf{a}_r\,|\,\rho_m} = \mathcal{O}(\varepsilon^p),\ p = 1,2,3\ldots$$

With these estimates, since the stiff medium is connected, we have again

$$L = \mathcal{O}\left(\frac{\Lambda_s}{2\pi}\right) = \mathcal{O}\left(\frac{1}{\omega}\sqrt{\frac{|\,\mathbf{a}_s\,|}{\rho_s}}\right) = \varepsilon^{-1}l, \quad \text{thus} \quad \rho_s\omega^2 = \varepsilon^2\frac{|\,\mathbf{a}_s\,|}{l^2}$$

and the wavelengths in constituents m and r are respectively of the order and significantly larger than the heterogeneity size

$$\frac{\Lambda_m}{2\pi} = \frac{1}{\omega}\sqrt{\frac{|\,\mathbf{a}_m\,|}{\rho_m}} = \mathcal{O}(l); \quad \frac{\Lambda_r}{2\pi} = \frac{1}{\omega}\sqrt{\frac{|\,\mathbf{a}_r\,|}{\rho_r}} = \mathcal{O}(\varepsilon^{-p/2}l).$$

Consequently, an inner-dynamics situation is expected within medium m (that contains inclusion r).

In addition, assuming the densities to be of the same order of magnitude

$$\frac{\rho_m}{\rho_s} = \frac{\rho_r}{\rho_s} = \mathcal{O}(1)$$

the contrasts of elastic properties are

$$\frac{|\,\mathbf{a}_m\,|}{|\,\mathbf{a}_s\,|} = \mathcal{O}(\varepsilon^2); \quad \frac{|\,\mathbf{a}_r\,|}{|\,\mathbf{a}_s\,|} = \mathcal{O}(\varepsilon^{2-p}), \quad p \geqslant 1.$$

The displacements in the three components are of similar order of magnitude. When using l as the characteristic length, the dimensionless equations that describe the wave propagation at constant frequency at the heterogeneity scales take the form (the notations for the dimensionless physical quantities are kept unchanged).

$$\mathrm{div}_y(\mathbf{a}_s : \mathbf{e}_y(\mathbf{u}_s)) = -\varepsilon^2\omega^2\rho_s\mathbf{u}_s \quad \text{within } \Omega_s, \tag{28}$$

$$\mathrm{div}_y(\mathbf{a}_m : \mathbf{e}_y(\mathbf{u}_m)) = -\omega^2\rho_m\mathbf{u}_m \quad \text{within } \Omega_m, \tag{29}$$

$$\mathrm{div}_y(\mathbf{a}_r : \mathbf{e}_y(\mathbf{u}_r)) = -\varepsilon^p\omega^2\rho_m\mathbf{u}_r \quad \text{within } \Omega_r, \tag{30}$$

with the boundary conditions

$$(\boldsymbol{\sigma}_s - \varepsilon^2\boldsymbol{\sigma}_m)\cdot\mathbf{n}_s = 0, \tag{31}$$

$$\mathbf{u}_s - \mathbf{u}_m = 0 \quad \text{over } \Gamma_s, \tag{32}$$

and

$$(\boldsymbol{\sigma}_r - \varepsilon^p\boldsymbol{\sigma}_m)\cdot\mathbf{n}_r = 0, \tag{33}$$

$$\mathbf{u}_r - \mathbf{u}_m = 0 \quad \text{over } \Gamma_r, \tag{34}$$

and the dimensionless momentum and moment of momentum balances of medium r are

$$\int_{\Omega_r}\rho_r\omega^2\,\mathbf{u}_r d\Omega = -\int_{\Gamma_r}\boldsymbol{\sigma}_m\cdot\mathbf{n}_r d\Omega, \tag{35}$$

$$\int_{\Omega_r}\rho_r\omega^2\mathbf{y}\wedge\mathbf{u}_r d\Omega = -\int_{\Gamma_r}\mathbf{y}\wedge\boldsymbol{\sigma}_m\cdot\mathbf{n}_r d\Omega. \tag{36}$$

3.2. Homogenization process

Introducing asymptotic expansions (9) into the above dimensionless heterogeneity scale model yields successive boundary value problems to be investigated.

3.2.1. Resolution in the stiff and connected media

It is clear that, at the three first orders, the momentum balance (28) and the boundary condition (31) yield similar results to Section 2.2 for medium s

$$\mathbf{u}_s^{(0)} = \mathbf{U}_s^{(0)}(\mathbf{x}), \tag{37}$$

$$\mathbf{u}_s^{(1)} = \boldsymbol{\chi}_s(\mathbf{y}) : \mathbf{e}_x(\mathbf{U}_s^{(0)}) + \mathbf{U}_s^{(1)}(\mathbf{x}), \tag{38}$$

$$\mathrm{div}_x(\mathbf{A}_s^{eff} : \mathbf{e}_x(\mathbf{u}_s^{(0)})) = -\omega^2 \langle \rho_s \rangle \mathbf{U}_s^{(0)} - \frac{1}{|\Omega|} \int_{\Gamma_s} (\mathbf{a}_m : \mathbf{e}_y(\mathbf{u}_m^{(0)})) \cdot \mathbf{n}_s \mathrm{d}\Gamma. \tag{39}$$

3.2.2. Resolution in the hard inclusion

Whatever $p \geqslant 1$, Eqs. (30) and (33) give at the first order for inclusion r (without periodicity condition since Ω_r is not connected)

$$\mathrm{div}_y(\mathbf{a}_r : \mathbf{e}_y(\mathbf{u}_r^{(0)})) = 0 \quad \text{within } \Omega_r,$$
$$(\mathbf{a}_r : \mathbf{e}_y(\mathbf{u}_r^{(0)})) \cdot \mathbf{n}_r = 0 \quad \text{over } \Gamma_r.$$

Therefore, the movement of inclusion r is a rigid motion at the first order of magnitude. However, since this medium is not connected, a rotation $\Omega^{(0)}$ is now permitted in addition to the differential translation $\widetilde{\mathbf{U}}_r^{(0)}$ (relatively to the stiff medium motion $\mathbf{U}_s^{(0)}$). Thus

$$\mathbf{u}_r^{(0)} = \mathbf{U}_s^{(0)}(\mathbf{x}) + \widetilde{\mathbf{U}}_r^{(0)}(\mathbf{x}) + \Omega_r^{(0)}(\mathbf{x}) \wedge \mathbf{y}, \tag{40}$$

where the origin of axes $\mathbf{y}$ is at the center of mass of inclusion r.

3.2.3. Resolution in the soft medium

Eqs. (29), (32) and (34) give at the order ε^0 an elasto-dynamic boundary value problem for $\mathbf{u}_m^{(0)}$

$$\mathrm{div}_y(\mathbf{a}_m : \mathbf{e}_y(\mathbf{u}_m^{(0)})) = -\omega^2 \rho_m \mathbf{u}_m^{(0)} \quad \text{within } \Omega_m, \tag{41}$$

$$\mathbf{u}_m^{(0)} = \mathbf{U}_s^{(0)}(\mathbf{x}) \quad \text{over } \Gamma_s, \tag{42}$$

$$\mathbf{u}_m^{(0)} = \mathbf{U}_s^{(0)}(\mathbf{x}) + \widetilde{\mathbf{U}}_r^{(0)}(\mathbf{x}) + \Omega_r^{(0)}(\mathbf{x}) \wedge \mathbf{y} \quad \text{over } \Gamma_r. \tag{43}$$

Let us introduce the auxiliary elasto-static problem

$$\mathrm{div}_y(\mathbf{a}_m : \mathbf{e}_y(\mathbf{w}_m^{(0)})) = 0 \quad \text{within } \Omega_m, \tag{44}$$

$$\mathbf{w}_m^{(0)} = \mathbf{U}_s^{(0)}(\mathbf{x}) \quad \text{over } \Gamma_s, \tag{45}$$

$$\mathbf{w}_m^{(0)} = \mathbf{U}_s^{(0)}(\mathbf{x}) + \widetilde{\mathbf{U}}_r^{(0)}(\mathbf{x}) + \Omega_r^{(0)}(\mathbf{x}) \wedge \mathbf{y} \quad \text{over } \Gamma_r. \tag{46}$$

Due to the linearity of the above system, we obtain

$$\mathbf{w}_m^{(0)}(\mathbf{y}) = \mathbf{U}_s^{(0)}(\mathbf{x}) + \boldsymbol{\mu}_m(\mathbf{y}) \cdot \widetilde{\mathbf{U}}_r^{(0)}(\mathbf{x}) + \boldsymbol{\nu}_m(\mathbf{y}) \cdot \Omega_r^{(0)}(\mathbf{x}), \tag{47}$$

where tensors $\boldsymbol{\mu}_m(\mathbf{y})$and $\boldsymbol{\nu}_m(\mathbf{y})$depend only on the elastic properties and on the geometry of medium m.

To investigate the boundary value problem (41)–(43), we put

$$\mathbf{u}_m^{(0)} = \mathbf{v} + \mathbf{w}_m^{(0)}.$$

The boundary value problem becomes

$$\mathrm{div}_y(\mathbf{a}_m : \mathbf{e}_y(\mathbf{v})) = -\omega^2 \rho_m (\mathbf{v} + \mathbf{w}_m^{(0)}(\mathbf{y})) \quad \text{within } \Omega_m, \tag{48}$$

$$\mathbf{v} = 0 \quad \text{over } \Gamma_s \text{ and } \Gamma_r. \tag{49}$$

Let us introduce the eigenvalue problem associated with the operator in the left hand member in (48), with the boundary conditions (49)

$$\mathrm{div}_y(\mathbf{a}_m : \mathbf{e}_y(\boldsymbol{\psi})) = -\eta \boldsymbol{\psi} \quad \text{within } \Omega_m,$$
$$\boldsymbol{\psi} = 0 \quad \text{over } \Gamma_s \text{ and } \Gamma_r.$$

The series of orthogonal eigenvectors $\{{}^i\boldsymbol{\psi}\}$ is associated to the discrete and positive series of eigenvalues $\{\eta_i\}$. Following the same reasoning as for the bi-composite, we deduce that

$$\mathbf{v} = \mathbf{u}_m^{(0)} - \mathbf{w}_m^{(0)} = \sum_{i=1}^{\infty} \frac{\langle \mathbf{w}_m^{(0)} \cdot {}^i\boldsymbol{\psi} \rangle_m}{\langle \|{}^i\boldsymbol{\psi}\|^2 \rangle_m} \frac{{}^i\boldsymbol{\psi}}{\frac{\eta_i}{\omega^2 \rho_m} - 1}. \tag{50}$$

Therefore, 48,49 have a solution when

$$\omega \neq \omega_i = \left(\frac{\eta_i}{\rho_m} \right)^{1/2}, \quad i = 1, 2 \ldots$$

If $\omega = \omega_i$, the solution exists when the corresponding vectorial eigenfunction ${}^i\boldsymbol{\psi}$ is orthogonal to $\mathbf{w}_m^{(0)}$ over Ω_m, i.e. if

$$\langle {}^i\boldsymbol{\psi} \cdot \mathbf{w}^{(0)} \rangle_m = 0.$$

When this condition is not met, $\mathbf{v}$ is not bounded in the vicinity of ω_i. Finally we obtain

$$\mathbf{u}_m^{(0)} = [\mathbf{I} + \boldsymbol{\beta}(\mathbf{y}, \omega)] \cdot \mathbf{U}_s^{(0)}(\mathbf{x}) + [\boldsymbol{\mu}_m(\mathbf{y}) + \boldsymbol{\gamma}(\mathbf{y}, \omega)] \cdot \widetilde{\mathbf{U}}_r^{(0)}(\mathbf{x}) + [\boldsymbol{\nu}_m(\mathbf{y}) + \boldsymbol{\delta}(\mathbf{y}, \omega)] \cdot \Omega_r^{(0)}(\mathbf{x}), \tag{51}$$

where $\boldsymbol{\beta}, \boldsymbol{\gamma}$ and $\boldsymbol{\delta}$ are second order tensors, depending on the frequency and on the elastic properties, the density and the geometry of medium m only. The expression of $\boldsymbol{\beta}$ and $\boldsymbol{\gamma}$ (for $\boldsymbol{\delta}$ replace $\boldsymbol{\mu}_m$ by $\boldsymbol{\nu}_m$ in γ) are given by

$$\boldsymbol{\beta}(\mathbf{y}) = \sum_{i=1}^{\infty} \frac{\langle {}^i\boldsymbol{\psi} \rangle_m \otimes {}^i\boldsymbol{\psi}}{\langle \|{}^i\boldsymbol{\psi}\|^2 \rangle_m} \frac{1}{\left(\frac{\omega_i}{\omega}\right)^2 - 1};$$

$$\boldsymbol{\gamma}(\mathbf{y}) = \sum_{i=1}^{\infty} \frac{\langle \boldsymbol{\mu}_m \cdot {}^i\boldsymbol{\psi} \rangle_m \otimes {}^i\boldsymbol{\psi}}{\langle \|{}^i\boldsymbol{\psi}\|^2 \rangle_m} \frac{1}{\left(\frac{\omega_i}{\omega}\right)^2 - 1}$$

3.2.4. Equivalent macroscopic description

The integral in the right hand member of (39) is calculated by integrating (41) over medium m, then by using the divergence theorem and finally Eq. (35)

$$\int_{\Gamma_s} (\mathbf{a}_m : \mathbf{e}_y(\mathbf{u}_m^{(0)})) \cdot \mathbf{n}_s \mathrm{d}\Gamma = -\int_{\Omega_m} \omega^2 \rho_m \mathbf{u}_m^{(0)} \mathrm{d}\Omega$$

$$-\int_{\Gamma_r} (\mathbf{a}_m : \mathbf{e}_y(\mathbf{u}_m^{(0)})) \cdot \mathbf{n}_s \mathrm{d}\Gamma = -\int_{\Omega_m} \omega^2 \rho_m \mathbf{u}_m^{(0)} \mathrm{d}\Omega - \int_{\Omega_r} \omega^2 \rho_r \mathbf{u}_r^{(0)} \mathrm{d}\Omega.$$

Introducing (51) into (39) and into (35) and (36) at the ε^0 order gives three equations for the equivalent macroscopic model of the three-constituent material

$$\mathrm{div}_x(\mathbf{A}_s^{eff} : \mathbf{e}_x(\mathbf{U}_s^{(0)})) = -\omega^2 \left(\mathbf{d}(\omega) \cdot \mathbf{U}_s^{(0)} + \mathbf{e}(\omega) \cdot \widetilde{\mathbf{U}}_r^{(0)} + \mathbf{f}(\omega) \cdot \Omega_r^{(0)} \right), \tag{52}$$

$$\omega^2 c_r \rho_r (\mathbf{U}_s^{(0)} + \widetilde{\mathbf{U}}_r^{(0)}) = \mathbf{g}(\omega) \cdot \mathbf{U}_s^{(0)} + \mathbf{h}(\omega) \cdot \widetilde{\mathbf{U}}_r^{(0)} + \mathbf{k}(\omega) \cdot \Omega_r^{(0)}, \tag{53}$$

$$\omega^2 \mathbf{J}_r \cdot \Omega_r^{(0)} = \mathbf{l}(\omega) \cdot \mathbf{U}_s^{(0)} + \mathbf{m}(\omega) \cdot \widetilde{\mathbf{U}}_r^{(0)} + \mathbf{n}(\omega) \cdot \Omega_r^{(0)}, \tag{54}$$

where tensors $\mathbf{d}(\omega), \mathbf{e}(\omega), \mathbf{f}(\omega)$ are given by, respectively,

$$\mathbf{d} = \langle \rho \rangle \mathbf{I} + \rho_m \langle \boldsymbol{\beta} \rangle_m, \quad \mathbf{e} = \rho_m \langle \boldsymbol{\mu}_m + \boldsymbol{\gamma} \rangle_m + \mathbf{c}_r \rho_r \mathbf{I},$$
$$\mathbf{f} = \rho_m \langle \boldsymbol{\nu}_m + \boldsymbol{\delta} \rangle_m.$$

Tensors $\mathbf{g}(\omega), \mathbf{h}(\omega), \mathbf{k}(\omega)$ are given by

$$\{\mathbf{g}, \mathbf{h}, \mathbf{k}\} = -\frac{1}{|\Omega|} \int_{\Gamma_r} (\mathbf{a}_m : \mathbf{e}_y(\mathbf{T}) \cdot \mathbf{n}_r \mathrm{d}\Omega); \quad \mathbf{T} = \{\boldsymbol{\beta}, \boldsymbol{\mu}_m + \boldsymbol{\gamma}, \boldsymbol{\nu}_m + \boldsymbol{\delta}\}.$$

Similarly, tensors $\mathbf{l}(\omega), \mathbf{m}(\omega), \mathbf{n}(\omega)$ are of the form

$$\{\mathbf{l}, \mathbf{m}, \mathbf{n}\} = -\int_{\Gamma_r} \mathbf{y} \wedge (\mathbf{a}_m : \mathbf{e}_y(\mathbf{T}) \cdot \mathbf{n}_r \mathrm{d}\Omega); \quad \mathbf{T} = \{\boldsymbol{\beta}, \boldsymbol{\mu}_m + \boldsymbol{\gamma}, \boldsymbol{\nu}_m + \boldsymbol{\delta}\}.$$

$\mathbf{J}_r$ is the inertial matrix of inclusion r.

Eqs. (53) and (54) are the reduced form of the dynamics of the system constituted by the soft medium (in local dynamic regime)

and the rigid inclusion (inducing additional inertial effect), which undergoes the uniform motion of the stiff medium. Hence, $\widetilde{\mathbf{U}}_{\mathrm{r}}^{(0)}$ and $\mathbf{U}_{\mathrm{r}}^{(0)}$ are linearly dependent on $\mathbf{U}_{\mathrm{s}}^{(0)}$ through frequency dependent tensors and can therefore be eliminated from (52).

After elimination, we obtain one equivalent macroscopic equation for the displacement $\mathbf{U}_{\mathrm{s}}^{(0)}$ in the form

$$\mathrm{div}_x(\mathbf{A}_{\mathrm{s}}^{eff} : \mathbf{e}_x(\mathbf{U}_{\mathrm{s}}^{(0)})) = -\omega^2 \boldsymbol{\rho}^{eff}(\omega) \cdot \mathbf{U}_{\mathrm{s}}^{(0)}. \tag{55}$$

Tensor $\mathbf{A}_{\mathrm{s}}^{eff}$ is the effective elastic tensor of constituent s defined in Section 2.2. This equation is similar to Eq. (18) for the two-constituent material, but the frequency dependent effective density $\boldsymbol{\rho}^{eff}$, of tensorial character, is different. Stopping bands are present in the vicinity of the eigenfrequencies of the soft medium/inclusion system. In dimensional form, the model becomes

$$\mathrm{div}_X(\mathbf{A}_{\mathrm{s}}^{eff} : \mathbf{e}_X(\mathbf{u}_{\mathrm{s}})) = -\omega^2 \boldsymbol{\rho}^{eff}(\omega) \cdot \mathbf{u}_{\mathrm{s}} + \mathcal{O}(\varepsilon).$$

3.2.5. Pure translation resonating system

If the system constituted by the soft medium and the inclusion presents three orthogonal common axes of symmetry (e. g. two centered ellipsoids or parallelepipeds with similar axes but with different aspect ratio), the rotational and translational modes are uncoupled. And since the system experiences a pure translation on its boundary, the inclusion does not rotate. The description reads, in this case

$$\mathrm{div}_x(\mathbf{A}_{\mathrm{s}}^{eff} : \mathbf{e}_x(\mathbf{U}_{\mathrm{s}}^{(0)})) = -\omega^2 \left(\mathbf{d}(\omega) \cdot \mathbf{U}_{\mathrm{s}}^{(0)} + \mathbf{e}(\omega) \cdot \widetilde{\mathbf{U}}_{\mathrm{r}}^{(0)}\right),$$
$$\omega^2 c_{\mathrm{r}} \rho_{\mathrm{r}} (\mathbf{U}_{\mathrm{s}}^{(0)} + \widetilde{\mathbf{U}}_{\mathrm{r}}^{(0)}) = \mathbf{g}(\omega) \cdot \mathbf{U}_{\mathrm{s}}^{(0)} + \mathbf{h}(\omega) \cdot \widetilde{\mathbf{U}}_{\mathrm{r}}^{(0)}.$$

The principal axes of tensors $\mathbf{d}, \mathbf{e}, \mathbf{g}, \mathbf{h}$, then of $\boldsymbol{\rho}^{eff}$, coincide with the symmetry axes. The principal values ρ_J^{eff} of the effective density tensor are given by

$$\rho_J^{eff} = \langle \rho \rangle + \rho_{\mathrm{m}} \langle \boldsymbol{\beta} \rangle_{\mathrm{mJ}} - (\rho_{\mathrm{m}} \langle \boldsymbol{\mu}_{\mathrm{m}} + \boldsymbol{\gamma} \rangle_{\mathrm{mJ}} + c_{\mathrm{r}} \rho_{\mathrm{r}}) \frac{g_J - \omega^2 c_{\mathrm{r}} \rho_{\mathrm{r}}}{h_J - \omega^2 c_{\mathrm{r}} \rho_{\mathrm{r}}}.$$

3.3. Soft constituent of weak density

We consider now a configuration where the soft medium is of weak density, where the estimates of the contrast of the other mechanical parameters are kept unchanged

$$\frac{\rho_{\mathrm{m}}}{\rho_{\mathrm{s}}} = \mathcal{O}(\varepsilon^q), \quad \frac{\rho_{\mathrm{r}}}{\rho_{\mathrm{s}}} = \mathcal{O}(1); \quad \frac{|\,\mathbf{a}_{\mathrm{m}}\,|}{|\,\mathbf{a}_{\mathrm{s}}\,|} = \mathcal{O}(\varepsilon^2), \quad \frac{|\,\mathbf{a}_{\mathrm{r}}\,|}{|\,\mathbf{a}_{\mathrm{s}}\,|} = \mathcal{O}(\varepsilon^{2-p});$$
$$q, p \geqslant 1.$$

Thus, the wavelengths in each constituents are significantly larger than the heterogeneity size

$$\frac{\Lambda_{\mathrm{s}}}{2\pi} = \varepsilon^{-1} l, ; \quad \frac{\Lambda_{\mathrm{m}}}{2\pi} = \mathcal{O}(\varepsilon^{-q/2} l); \quad \frac{\Lambda_{\mathrm{r}}}{2\pi} = \mathcal{O}(\varepsilon^{-p/2} l).$$

In this case, the set of dimensionless governing equations is given by (28)–(36) except for the momentum balance of medium m (29) that becomes

$$\mathrm{div}_y(\mathbf{a}_{\mathrm{m}} : \mathbf{e}_y(\mathbf{u}_{\mathrm{m}})) = -\varepsilon^q \omega^2 \rho_{\mathrm{m}} \mathbf{u}_{\mathrm{m}} \quad \text{within } \Omega_{\mathrm{m}},$$

As medium m is now locally in a quasi-static state, $\mathbf{u}_{\mathrm{m}}^{(0)}(\mathbf{y})$ is simply defined by (47)

$$\mathbf{u}_{\mathrm{m}}^{(0)}(\mathbf{y}) = \mathbf{w}_{\mathrm{m}}^{(0)}(\mathbf{y}) = \mathbf{U}_{\mathrm{s}}^{(0)}(\mathbf{x}) + \boldsymbol{\mu}_{\mathrm{m}}(\mathbf{y}) \cdot \widetilde{\mathbf{U}}_{\mathrm{r}}^{(0)}(\mathbf{x}) + \boldsymbol{\nu}_{\mathrm{m}}(\mathbf{y}) \cdot \Omega_{\mathrm{r}}^{(0)}(\mathbf{x}).$$

Furthermore, the negligible inertia of medium m implies

$$\int_{\Gamma_{\mathrm{s}}} (\mathbf{a}_{\mathrm{m}} : \mathbf{e}_y(\mathbf{u}_{\mathrm{m}}^{(0)})) \cdot \mathbf{n}_{\mathrm{s}} \, \mathrm{d}\Gamma = -\int_{\Gamma_{\mathrm{r}}} (\mathbf{a}_{\mathrm{m}} : \mathbf{e}_y(\mathbf{u}_{\mathrm{m}}^{(0)})) \cdot \mathbf{n}_{\mathrm{s}} \mathrm{d}\Gamma$$
$$= -\int_{\Omega_{\mathrm{r}}} \omega^2 \rho_{\mathrm{r}} \mathbf{u}_{\mathrm{r}}^{(0)} \mathrm{d}\Omega.$$

Consequently, the macroscopic description reads

$$\mathrm{div}_x(\mathbf{A}_{\mathrm{s}}^{eff} : \mathbf{e}_x(\mathbf{U}_{\mathrm{s}}^{(0)})) = -\omega^2 (\langle \rho \rangle \mathbf{U}_{\mathrm{s}}^{(0)} + c_{\mathrm{r}} \rho_{\mathrm{r}} \widetilde{\mathbf{U}}_{\mathrm{r}}^{(0)}), \tag{56}$$
$$\omega^2 c_{\mathrm{r}} \rho_{\mathrm{r}} (\mathbf{U}_{\mathrm{s}}^{(0)} + \widetilde{\mathbf{U}}_{\mathrm{r}}^{(0)}) = \mathbf{h}' \cdot \widetilde{\mathbf{U}}_{\mathrm{r}}^{(0)} + \mathbf{k}' \cdot \Omega_{\mathrm{r}}^{(0)}, \tag{57}$$
$$\omega^2 \mathbf{J}_{\mathbf{r}} \cdot \Omega_{\mathrm{r}}^{(0)} = \mathbf{m}' \cdot \widetilde{\mathbf{U}}_{\mathrm{r}}^{(0)} + \mathbf{n}' \cdot \Omega_{\mathrm{r}}^{(0)}, \tag{58}$$

where tensors $\mathbf{h}', \mathbf{k}', \mathbf{m}', \mathbf{n}'$ are *independent* of the frequency and involve the elastic properties and the geometry of medium m only. Their expressions are respectively

$$\{\mathbf{h}', \mathbf{k}'\} = -\frac{1}{|\,\Omega\,|} \int_{\Gamma_{\mathrm{r}}} (\mathbf{a}_{\mathrm{m}} : \mathbf{e}_y(\mathbf{T}) \cdot \mathbf{n}_{\mathrm{r}} \mathrm{d}\Omega; \quad \mathbf{T} = \{\boldsymbol{\mu}_{\mathrm{m}}, \boldsymbol{\nu}_{\mathrm{m}}\},$$
$$\{\mathbf{m}', \mathbf{n}'\} = -\int_{\Gamma_{\mathrm{r}}} \mathbf{y} \wedge (\mathbf{a}_{\mathrm{m}} : \mathbf{e}_y(\mathbf{T})) \cdot \mathbf{n}_{\mathrm{r}} \mathrm{d}\Omega; \quad \mathbf{T} = \{\boldsymbol{\mu}_{\mathrm{m}}, \boldsymbol{\nu}_{\mathrm{m}}\}.$$

Eqs. (57) and (58) express the dynamics of the system constituted by the soft medium (in local quasi-static regime) and the hard inclusion (introducing the inertial effect), undergoing the uniform motion of the stiff medium. Note that the soft medium/hard inclusion system simply reduces to a six degrees of freedom (dof) oscillator governed by the elasticity of domain m (of negligible mass) and the inertia of inclusion r. After elimination of $\widetilde{\mathbf{U}^{(0)}}_{\mathrm{r}}$ and $\boldsymbol{\Omega}_{\mathrm{r}}^{(0)}$ between the three above equations, we obtain once again the macroscopic equation in the form

$$\mathrm{div}_x(\mathbf{A}_{\mathrm{s}}^{eff} : \mathbf{e}_x(\mathbf{U}_{\mathrm{s}}^{(0)})) = -\omega^2 \boldsymbol{\rho}^{eff}(\omega) \cdot \mathbf{U}_{\mathrm{s}}^{(0)}, \tag{59}$$

This equation is formally similar to Eq. (18). The difference lies in the finite number of eigenmodes (6 dof at the most) which generates the singularities of $\boldsymbol{\rho}^{eff}$. Hence, in the studied frequency range, only a finite number of stopping bands occurs. The higher modes involving the dynamics of medium m appear at significantly higher frequencies, for which

$$\frac{\Lambda_{\mathrm{m}}}{2\pi} = \mathcal{O}(l) \quad \text{thuss} \quad \frac{\Lambda_{\mathrm{s}}}{2\pi} = \varepsilon^{-1+q/2} l$$

and correspond to homogenizable situations if $q = 1$, only.

The eigenmodes are evidenced simply when considering sufficiently symmetric domains $\boldsymbol{\Omega}_{\mathrm{m}}$and $\boldsymbol{\Omega}_{\mathrm{r}}$ to have uncoupled translational and rotational modes. Then $\mathbf{k}' = \mathbf{0}$ (and $\mathbf{m}' = \mathbf{0}$ also by Maxwell–Betti reciprocity), the principal axes of the elastic tensor $\mathbf{h}'$ and of the effective density tensor $\boldsymbol{\rho}^{eff}$ coincide, and their three eigenvalues (index j) are simply related by

$$\rho_j^{eff}(\omega) = \langle \rho \rangle + \frac{c_{\mathrm{r}} \rho_{\mathrm{r}}}{(\frac{\omega_j}{\omega})^2 - 1}; \quad \omega_j^2 = \frac{h_j'}{c_{\mathrm{r}} \rho_{\mathrm{r}}}; \quad j = 1, 2, 3.$$

Note that if medium m presents a viscoelastic behavior characterized by a complex tensor $\mathbf{a}_{\mathrm{m}}^* = (1 + i\xi)\mathbf{a}_{\mathrm{m}}, h_j'$ have to be replaced by $h_j^* = h_j'(1 + i\xi)$ in the previous expression.

4. Examples and discussion

To illustrate the three analyzed configurations, let us consider highly contrasted stratified composites made of isotropic elastic plates. The symmetric period of zero axial thickness ($\{\frac{c_{\mathrm{s}} l}{2}, \frac{c_{\mathrm{m}} l}{2}, c_{\mathrm{r}} l, \frac{c_{\mathrm{m}} l}{2}, \frac{c_{\mathrm{s}} l}{2}\}$, see Fig. 4) corresponds to the configuration and material properties presented in Section 3.1 with $q = 1$. The bi-composite material (Section 2) and tri-composite material (Section 3.3) will be obtained by taking $c_{\mathrm{r}} = 0$ and $\rho_{\mathrm{m}} = 0$ respectively. In such stratified media, the stiff constituent is connected along any directions in the plane of the layers and is able to carry long compressional waves propagating in these directions (e.g. axial direction $\mathbf{e}_1$). The soft layers are submitted to a shear forced vibration initiated by the stiff layers, which propagates in the direction perpendicular to the layers. Further, the symmetry of the period imposes that the motions (i) are polarized along $\mathbf{e}_1$, (ii) vary at

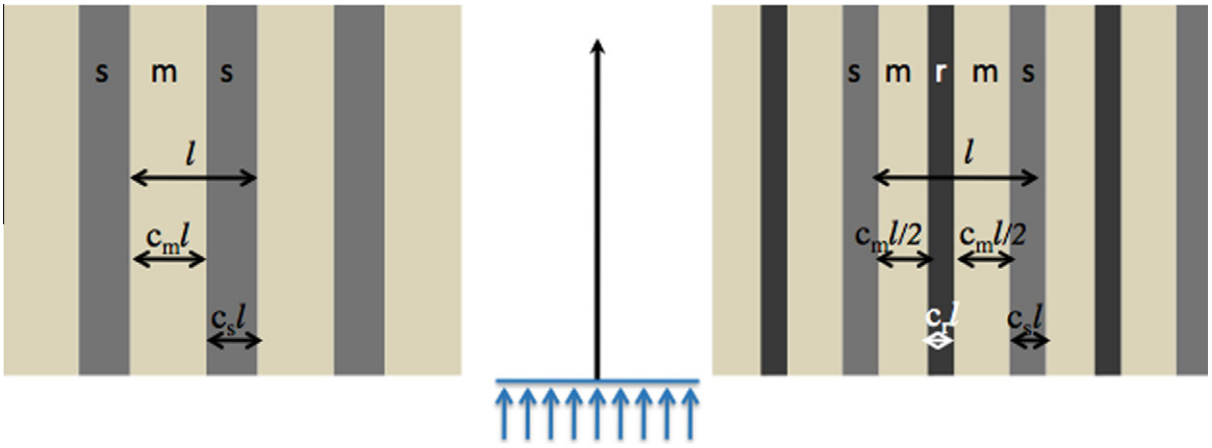

Fig. 4. Bi and tri-stratified composites under macroscopic compression wave. Note that within a plane wave, the motion of the stiff medium is uniform and coincide with the macroscopic motion; conversely, the motion of the soft layer is non uniform due to the inner shear resonance and differ from the macroscopic motion, see (61).

the macroscale according to the axial variable x_1 and (iii) depend at the local scale on the variable normal to the plate (say variable y_2 along $\mathbf{e}_2$). As seen previously, the stiff layer works as in absence of the soft medium, hence as an isolated plate with an in plane compression $E_s/(1-\nu_s^2)$, where E_s is the Young modulus and ν_s the Poisson ratio. Thus, the in-plane elastic compression coefficient A_s^{eff} of the stratified composite is

$$A_s^{eff} = c_s \frac{E_s}{1-\nu_m^2}$$

At the scale of the period the motion of the stiff medium is uniform i.e. $u_s = U_s(x_1)\mathbf{e}_1$. Conversely, under the imposed motion $U_s(x_1)\mathbf{e}_1$ at its boundary, the soft medium experiences a non-uniform motion $u_m(x_1, y_2)$. This latter is governed by the set (41)–(43). In the present case it expresses the balance between the inertial vertical forces and the shear forces involved in the non uniform field. The differential set reduces to a single equation that describes the shear forced vibration which propagates in the direction perpendicular to the layers (where μ_m denotes shear modulus, and ' denotes the derivative $\frac{d}{dy_2}$):

$$\mu_m u_m'' + \omega^2 \rho_m u_m = 0,$$

with the boundary conditions

$$u_m(x_1, y_2 = 0) = U_s(x_1); \quad u_m(x_1, y_2 = \frac{c_m l}{2}) = U_s(x_1) + \widetilde{U}_r(x_1)$$

and the equilibrium condition of the rigid included plate of medium r:

$$\mu_m u_m'\left(x_1, \frac{c_m l}{2}\right) = \omega^2 \rho_r \widetilde{U}_r(x_1) \frac{c_r l}{2}.$$

We deduce that:

$$u_m(x_1, y_2) = (R\sin(\alpha y_1) + \cos(\alpha y_1))U_s(x_1), \tag{60}$$

$$\widetilde{U}_r(x_1) = \left(-1 + \frac{1}{C}\frac{1}{1 - T\frac{\omega^2\rho_r}{\mu_m}\frac{c_r l}{2\alpha}}\right)U_s(x_1), \tag{61}$$

where

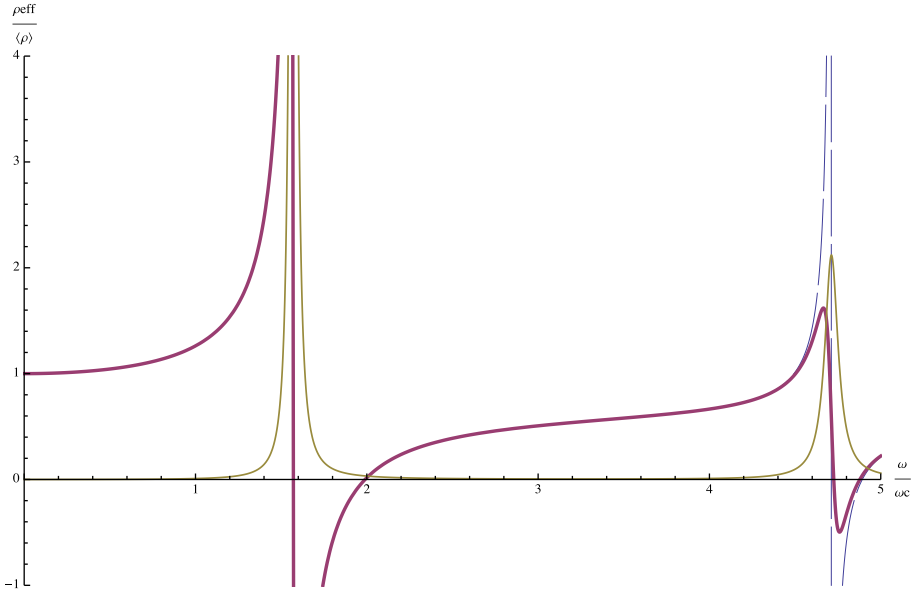

Fig. 5. Effective normalized density of concrete/silicon stratified material versus normalized frequency calculated from Eq. (64) with material properties defined in the text. Dashed line: elastic case; bold line and normal line: real and imaginary part, respectively, in visco-elastic case ($\xi = 0.01$).

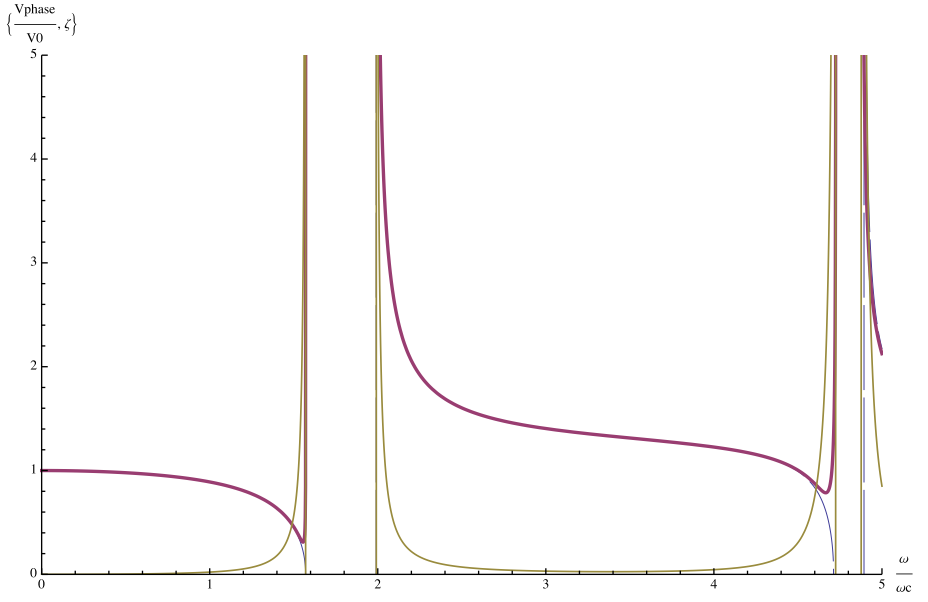

Fig. 6. Normalized phase velocity and attenuation per wavelength of Concrete/Silicon stratified material versus normalized frequency. Same legend as in Fig. 5. Note the quasi coincidence of the phase velocities in elastic and viscoelastic cases.

$$\alpha = \omega\sqrt{\frac{\rho_m}{\mu_m}};\quad T = \tan\left(\alpha\frac{c_m l}{2}\right);\quad C = \cos\left(\alpha\frac{c_m l}{2}\right);$$
$$R = \frac{T + \frac{\omega^2\rho_r}{\mu_m}\frac{c_r l}{2\alpha}}{1 - T\frac{\omega^2\rho_r}{\mu_m}\frac{c_r l}{2\alpha}}.$$

Consequently, for a general tri-composite as in Section 3.1, the effective density reads,:

$$\rho^{eff}(\omega) = c_s\rho_s + c_m\rho_m\left(\frac{TC}{\alpha\frac{c_m l}{2}} + R\frac{1-C}{\alpha\frac{c_m l}{2}}\right) + \frac{c_r\rho_r}{C}\frac{1}{1 - T\frac{\omega^2\rho_r}{\mu_m}\frac{c_r l}{2\alpha}}. \quad (62)$$

Thus, the phase wave velocity and its normalized value are respectively given by:

$$V(\omega) = \sqrt{\frac{c_s E_s}{(1-\nu_m^2)\rho^{eff}(\omega)}};\quad \frac{V(\omega)}{V(0)} = \sqrt{\frac{\langle\rho\rangle}{\rho^{eff}(\omega)}}.$$

The inner-resonance band gaps correspond to negative values or very large values of the effective density $\rho^{eff}(\omega)$. Each band gap is associated with a pole of $\rho^{eff}(\omega)$defined by the roots of:

$$\tan\left(\alpha\frac{c_m l}{2}\right)\frac{c_m l}{2\alpha} = \frac{c_m\mu_m}{\omega^2 c_r\rho_r}.$$

For visco-elastic media, $V(\omega)$ is complex and the phase velocity $V_{phase}(\omega)$ and the damping per wavelength ζ are respectively given by:

$$V_{phase}(\omega) = \frac{|V(\omega)|^2}{Re(V(\omega))};\quad \zeta = -2\pi\frac{Im(V(\omega))}{Re(V(\omega))}.$$

For a tri-composite as in Section 3.3, one obtains (by taking the limit $\alpha \to 0$ in (62))

$$\rho^{eff}(\omega) = c_s\rho_s + \frac{c_r\rho_r}{1 - \left(\frac{\omega}{\omega_0}\right)^2};\quad \omega_0 = \sqrt{\frac{\mu_m}{\rho_r}}\frac{2}{\sqrt{c_m c_r}l} \quad (63)$$

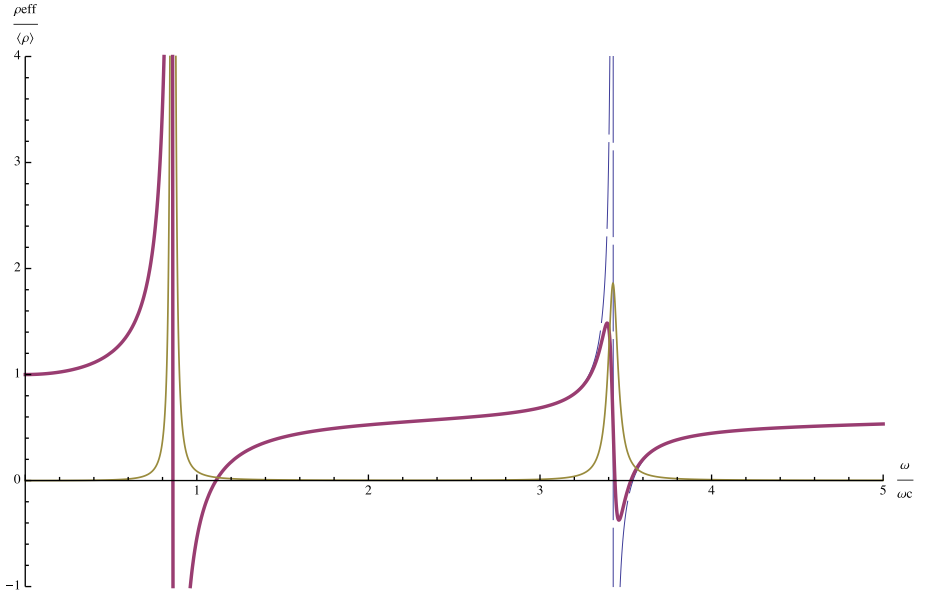

Fig. 7. Effective normalized density versus normalized frequency of concrete/silicone/epoxy stratified material derived from Eq. (62). Same legend as in Fig. 5.

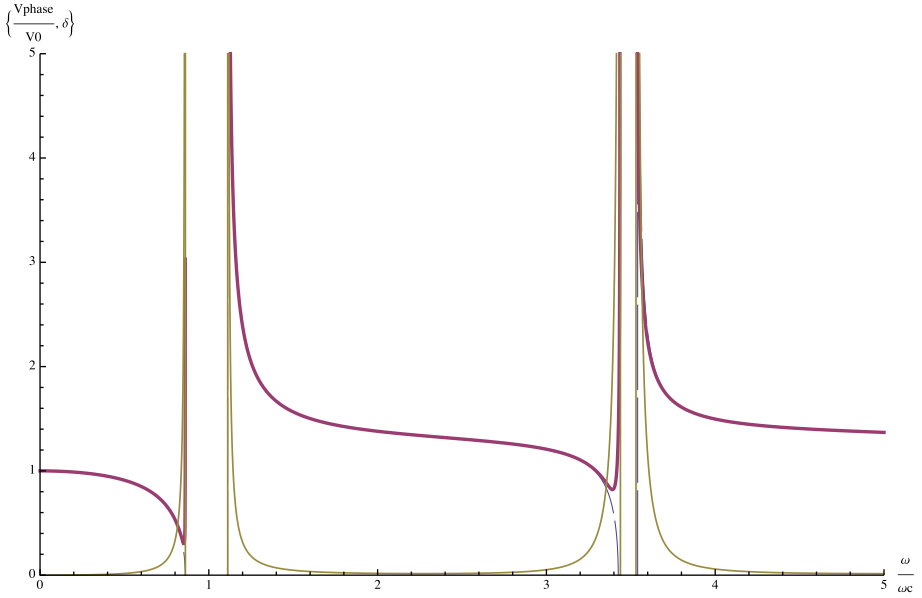

Fig. 8. Normalized phase velocity and attenuation per wavelength of concrete/silicon/epoxy stratified material versus normalized frequency. Same legend as in Fig. 5.

and the pole ω_0 is related to the unique inner-resonance band gap (in the frequency range respecting the scale separation).

Finally, for a bi-composite as in Section 2 (i.e., taking $c_r = 0$ in (62)),

$$\rho^{eff}(\omega) = c_s\rho_s + c_m\rho_m \frac{T}{\alpha \frac{c_m l}{2}} \tag{64}$$

and the series of poles associated to the inner-resonance band gaps satisfy:

$$\cos\left(\alpha \frac{c_m l}{2}\right) = 0; \quad \text{i.e.} \quad \omega_k^2 = \sqrt{\frac{\mu_m}{\rho_m}} \frac{(1+2k)\pi}{c_m l}.$$

In practice, bi-stratified composites could be realized with high performance concrete ($E_s \approx 6 \times 10^{10}$ Pa, $\rho_s \approx 2.7 \times 10^3$ kg/m^3, $\nu_s = 0.2$) and silicone ($\mu_m \approx 5 \times 10^5$ Pa, $\rho_m \approx 1.2 \times 10^3$ kg/m^3). Regarding tri-stratified composites as in Section 3.1, an epoxy layer ($\mu_r \approx 5 \times 10^9$ Pa, $\rho_r \approx 1.2 \times 10^3$ kg/m^3) can be inserted in the silicone, and, to obtain composites as in Section 3.3, one can replace the silicone by a polyurethane foam ($\mu_m \approx 1.2 \times 10^5$ Pa, $\rho_m \approx 60$ kg/m^3).

Fig. 5 depicts the variation of $\rho_j^{eff}(\omega)/\langle\rho\rangle$ versus the normalized angular frequency ω/ω_c with $\omega_c = \omega\sqrt{\frac{\rho_m}{\mu_m}} c_s l/2$, for a concrete/silicon bi-composite material where $c_s = 1/3$, $c_m = 2/3$ without or with damping ($\xi = 0.01$). For the same media, Fig. 6 presents the normalized phase velocity $V_{phase}/V(0)$ and the damping per wavelength ζ.

The importance of the resonating effect and the smoothing induced by damping is clearly evidenced. For pure elastic constituents, the effective density defines the band gaps as the frequency interval between null velocity ($\rho^{eff}(\omega) \to \infty$) and infinite velocity

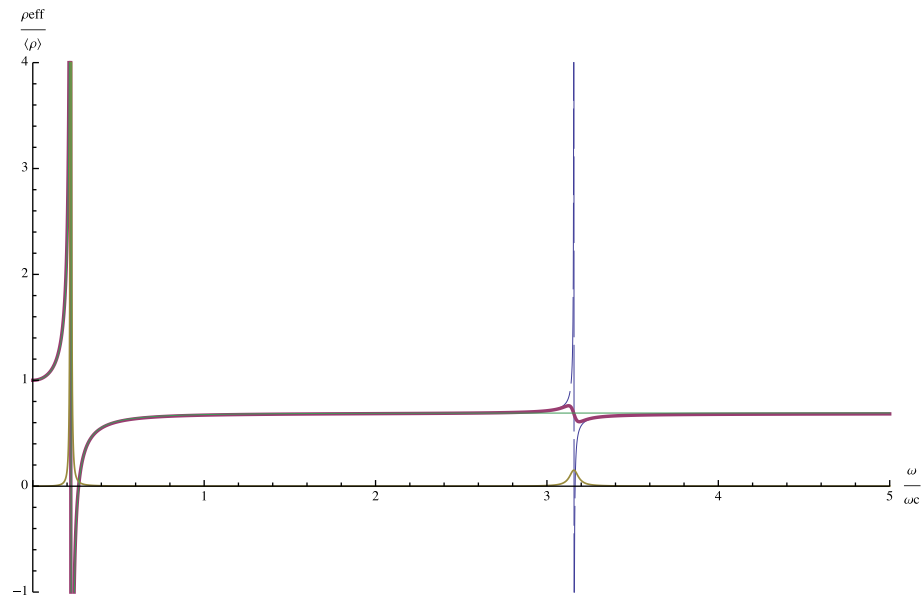

Fig. 9. Effective normalized density versus normalized frequency of concrete/foam/epoxy stratified material derived from Eq. (62). Same legend as in Fig. 5. Further, the bold dashed line corresponds to the real part given by Eq. (63) in presence of damping. Note the perfect agreement of both results for the fundamental mode and the slight discrepancy around the second mode that is disregarded in (63).

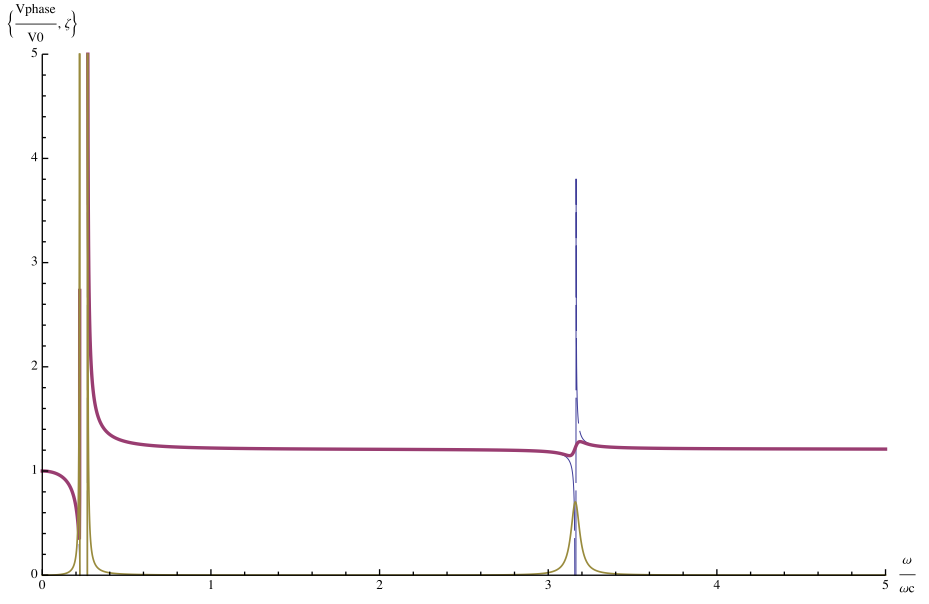

Fig. 10. Normalized phase velocity and attenuation per wavelength of concrete/silicon/epoxy stratified material versus normalized frequency. Same legend as in Fig. 5.

($\rho^{eff}(\omega) = 0$). In the viscoelastic case, the phase velocity is almost identical to the elastic case one in the whole frequency range (except in the very vicinity of band gaps). The main difference lies in the attenuation effect that is very significant around the band gaps. In practice this leads to enlarge the width of the band gap.

Figs. 7 and 8 display the same parameters for a concrete/silicon/epoxy tri-composite material with $c_s = c_m = c_r = 1/3$; Figs. 9 and 10 correspond to the same tri-composite material except that silicon is replaced by foam. These different cases present the same general trends. However the dynamic responses significantly differ according to the considered media. Composite materials based on 3D cells exhibit phenomena of the same nature as those evidenced on these stratified media, but their accurate description requires dynamic calculations on the microstructure. Nevertheless, a rough analysis is possible from simple approaches: the effective elastic tensor $\mathbf{A}_s^{eff}$ can be assessed through a generalized self-consistent approach Christensen and Lo, 1979 (by considering constituent s only, provided that c_s is not too weak, say $c_s \geqslant 0.1$), and the fundamental frequency of the inner resonance can be approximated from proper geometric simplifications (concentric spheres, "concentric" parallelepipeds, plates in cubes, ...).

5. Conclusion

The above study evidences that the requirements for the occurrence of inner resonance phenomena in highly contrasted composite materials can be summarized as follows:

- The stiff constituent acts as the carrying structure for the long wavelength. This entails (i) that this constituent must be connected (at least along the wave propagation direction) and (ii) that the frequency range is such that the wavelength in this constituent is large with respect to the period size l, $\Lambda_s/2\pi l = \varepsilon \ll 1$.
- Within this frequency range, the soft medium – which can itself contain hard unconnected inclusions - reaches its own resonant states and acts as a resonating system.
- To actually have these very distinct roles of the constituents (carrying and resonating), a stiffness contrast $|\mathbf{a}_m| / |\mathbf{a}_s| = \mathcal{O}(\varepsilon^2)$ is necessary.
- Finally, when the mean density of the whole resonating system (homogeneous or heterogeneous) is of the order of that of the carrying structure, the composite material behaves as a "metamaterial".

The specificity of this situation lies in the fact that the effective density differs from the real density. The composite material shows generally a series of inner-resonance cut-off frequencies, that may reduce to a few frequencies in some particular cases. Each band gap is associated to an eigenvalue problem of the resonating system with a homogeneous Dirichlet condition on the boundary with the "carrying" medium, whatever its geometry is. If several unconnected resonating domains are present in a period (a REV), each of them introduces its own cut-off frequencies related to its resonant states. Recall that, conversely to high-frequency band gaps strictly related to the periodicity of the media, the band gaps induced by inner-resonance at large wavelength occurs even in non periodic media that present a REV.

As the present work focuses on local resonance while the scale separation is satisfied, the phenomena differs (i) from Rayleigh scattering in usual composite materials (where wavelengths are not very large compared to the period, hence when local dynamic effects are weak) Boutin and Auriault, 1993, and (ii) from Bragg scattering, which appears in high frequency phonic crystals (when wavelengths are comparable to the period size). In this latter case, the homogenization approach is inoperative, but periodic media can be described through Floquet–Bloch approach (Turbe, 1982; Allaire and Conca, 1998).

It is worth noticing that the situation of local resonance in highly contrasted elastic composite materials evidenced by Auriault and Bonnet (1985) belongs to the wider class of macro phenomena evolving out of equilibrium local state. For instance, similar mechanisms appear in double conductivity media (Auriault, 1983) and double porosity media (Auriault and Boutin, 1994) and were experimentally proved in poroacoustics (Olny and Boutin, 2003). In these latter cases, the difference with elastic composites lies in the fact that the resonance concerns a diffusion phenomenon (related to thermal transfer or mass transfer driven by viscous effect). Undamped resonance (elastic cases) or damped

resonance (diffusion cases) yield different macroscopic modeling (with or without inner-resonance cut-off frequencies respectively). However, their common feature is that they lead at the macroscopic scale to a generalized Newtonian mechanics, in the sense that the effective mass density (or thermal inertia, etc.) differs from the real mass density and is frequency dependent.

References

Allaire, G., Conca, C., 1998. Bloch wave homogenization and spectral asymptotic analysis. J. Math. Pures Appl. 77, 153–208.

Auriault, J.-L., 1983. Effective macroscopic description for heat conduction in periodic composites. Int. J. Heat Mass Transf. 26 (6), 861–869.

Auriault, J.-L., 1991. Heterogeneous medium. Is an equivalent description possible? Int. J. Eng. Sci. 29 (7), 785–795.

Auriault, J.-L., 1994. Acoustics of heterogeneous media: macroscopic behavior by homogenization. Curr. Topics Acoust. Res. I, 63–90.

Auriault, J.-L., 2011. Heterogeneous periodic and random media. Are the equivalent macroscopic descriptions similar? IJES 49, 806–808.

Auriault, J.-L., Bonnet, G., 1985. Dynamique des composites élastiques périodiques. Arch Mech. 37 (4–5), 269–284 (in French).

Auriault, J.L., Boutin, C., 1994. Deformable porous media with double porosity. III Acoustics. Transport in Porous Media 14, 143–162.

Auriault, J.-L., Boutin, C., Geindreau, C., 2009. Homogenization of Coupled Phenomena in Heterogenous Media. ISTE and Wiley.

Ávila, A., Griso, G., Miara, B., 2005. Bandes phoniques interdites en élasticité linéarisée. C.R. Acad. Sci. Paris, Ser. I 340, 933–938.

Babych, N.O., Kamotski, I.V., Smyshlyaev, V.P., 2008. Homogenization of spectral problems in bounded domains with doubly high contrasts. Netw. Heterogen. Media 3 (3), 413–436.

Bensoussan, A., Lions, J.-L., Papanicolaou, G., 1978. Asymptotic Analysis for Periodic Structures. North Holland, Amsterdam.

Boutin, C., Auriault, J.-L., 1993. Rayleigh scattering in elastic composite materials. Int. J. Eng. Sci. 31 (12), 1669–1689.

Boutin, C., Hans, S., Chesnais, C., 2010. Generalized beam and continua. Dynamics of reticulated structures. In: Maugin, G.A., Metrikine, A.V. (Eds.), Mechanics of Generalized Continua. Springer, New York, pp. 131–141.

Christensen, R.M., Lo, K.H., 1979. Solution for effective shear properties in three-phase sphere and cylinder models. J. Mech. Phys. Solid 27, 315–330.

Courant, R., Hilbert, D., 1970. Methods of Mathematical Physics I. eighth ed.. Interscience publishers Inc., New York.

Léné, F., 1978. 'Comportement macroscopique de matériaux élastiques comportant des inclusions rigides ou des trous répartis périodiquement'. C.R. Acad. Sci. Paris, Ser. IIB 286, 75–78.

Liu, Z., Zhang, X., Mao, Y., Zhu, Y.Y., Yang, Z., Chan, C.T., Sheng, P., 2000. Locally resonant materials. Science 289, 1734–1736.

Liu, Z., Chan, C.T., Sheng, P., 2005. 'Analytic model of phononic crystals with local resonance'. Phys. Rev. B 71, 014103.

Milton, G.W., Willis, J.R., 2007. On modifications of Newton's second law and linear continuum elastodynamics. Proc. R. Soc. A 463, 855–880.

Olny, X., Boutin, C., 2003. Acoustic wave propagation in double porosity media. J.A.S.A. 113 (6), 73–89.

Sanchez-Palencia, E., 1980. Non-Homogeneous Media and Vibration theory. Springer-Verlag, Berlin.

Sheng, P., Zhang, X.X., Liu, Z., Chan, C.T., 2003. Locally resonant sonic materials. Physica B 338, 201–205.

Smyshlyaev, V.P., 2009. 'Propagation and localization of elastic waves in highly anisotropic periodic composites via two-scale homogenization'. Mech. Mater. 41 (4), 434–447.

Turbe, N., 1982. Application of Bloch expansion to periodic elastic and viscoelastic media. Math. Methods Appl. Sci. 4 (4–5), 433–449.

Vasseur, J.O., Deymier, P.A., Prantziskonis, G., Hong, G., 1998. Experimental evidence for the existence of absolute acoustic band gaps in two-dimensional periodic composite media. J. Phys.: Condens. Mater. 10, 6051–6064.

Zhikov, V.V., 2000. On an extension of the method of two-scale convergence and its applications. Sbor. Math. 191 (7–8), 973–1014.